

# Solving SU(3) Yang-Mills theory on the lattice: a calculation of selected gauge observables with gradient flow

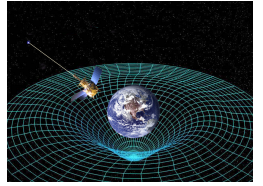
---

Hans Mathias Mamen Vege  
04.07.19

Supervisor: *Andrea Shindler*  
Co-supervisor: *Morten Hjorth-Jensen*

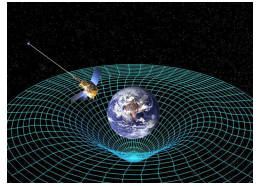
University of Oslo

# The four forces of nature



Gravity

# The four forces of nature

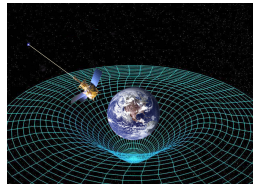


Gravity



Electromagnetism

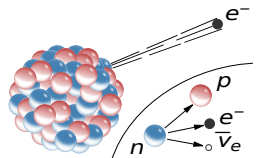
# The four forces of nature



Gravity

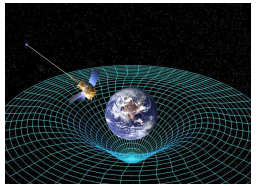


Electromagnetism



Weak nuclear force

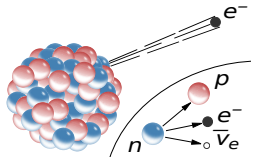
# The four forces of nature



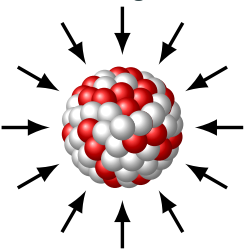
Gravity



Electromagnetism



Weak nuclear force



Strong nuclear force

## What is the strong force?

The mass discrepancy is due to the interaction energy in which gluons are mediators.

Consists of:

- 6 quark flavors: up, down, strange, charm, bottom and top

## What is the strong force?

The mass discrepancy is due to the interaction energy in which gluons are mediators.

Consists of:

- 6 quark flavors: up, down, strange, charm, bottom and top
- 8 gluons

## What is the strong force?

The mass discrepancy is due to the interaction energy in which gluons are mediators.

Consists of:

- 6 quark flavors: up, down, strange, charm, bottom and top
- 8 gluons

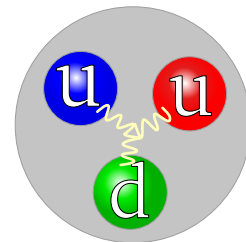
## What is the strong force?

The mass discrepancy is due to the interaction energy in which gluons are mediators.

Consists of:

- 6 quark flavors: up, down, strange, charm, bottom and top
- 8 gluons

A proton consists of: up-, up- and down-quarks



## What is the strong force?

The mass discrepancy is due to the interaction energy in which gluons are mediators.

Consists of:

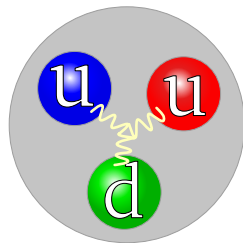
- 6 quark flavors: up, down, strange, charm, bottom and top
- 8 gluons

A **proton** consists of: up-, up- and down-quarks

Mass discrepancy:

$$m_p \neq m_u + m_u + m_d,$$

$$936 \text{ MeV} \neq 3 \text{ MeV} + 3 \text{ MeV} + 6 \text{ MeV}.$$



## Comparing the strong force and QED

Electromagnetism or Quantum Electrodynamics(QED), a U(1) symmetry theory:

$$\mathcal{L}_{\text{QED}} = \sum_{f=\text{fermions}} \bar{\psi}_f (i\gamma^\mu (\partial_\mu + ieQ_f A_\mu) - m_f) \psi_f - \frac{1}{4} F_{\mu\nu} F^{\mu\nu}$$

Field strength tensor:

$$F_{\mu\nu} = \partial_\mu A_\nu - \partial_\nu A_\mu$$

- QED is U(1) theory, and the simply means that it contains a simple rotational symmetry.
- $e$  is the coupling constant and  $Q_f$  is the charge.
- $\bar{\psi}_f$  and  $\psi_f$  are is the fermion fields.
- $A_\mu$  is the gauge fields.
- $\gamma^\mu$  is the Dirac matrices.
- First part contains the dynamics of all the fermions such as electrons, muons ect.
- Second part contains the dynamics of the photon fields in terms of the field strength tensor.

## Comparing the strong force and QED

Electromagnetism or Quantum Electrodynamics(QED), a U(1) symmetry theory:

$$\mathcal{L}_{\text{QED}} = \sum_{f=\text{fermions}} \bar{\psi}_f (i\gamma^\mu (\partial_\mu + ieQ_f A_\mu) - m_f) \psi_f - \frac{1}{4} F_{\mu\nu} F^{\mu\nu}$$

Field strength tensor:

$$F_{\mu\nu} = \partial_\mu A_\nu - \partial_\nu A_\mu$$

The **strong nuclear force** or Quantum Chromo Dynamics(QCD), a SU(3) symmetry theory:

$$\mathcal{L}_{\text{QCD}} = \sum_{f=u,d,\dots} \bar{\psi}_f (i\gamma^\mu (\partial_\mu + ig_s A_\mu^a T^a) - m_f) \psi_f - \frac{1}{4} G_{\mu\nu}^a G^{a\mu\nu}$$

Field strength tensor:

$$G_{\mu\nu}^a = \partial_\mu A_\nu^a - \partial_\nu A_\mu^a - g_s f^{abc} A_\mu^b A_\nu^c$$

- QED is U(1) theory, and the simply means that it contains a simple rotational symmetry.

- $e$  is the coupling constant and  $Q_f$  is the charge.

- $\bar{\psi}_f$  and  $\psi_f$  are is the fermion fields.

- $A_\mu$  is the gauge fields.

- $\gamma^\mu$  is the Dirac matrices.

- First part contains the dynamics of all the fermions such as electrons, muons ect.

- Second part contains the dynamics of the photon fields in terms of the field strength tensor.

- Instead of a sum over all fermions, it is a sum over all quarks.

- The coupling constant is now the strong coupling,  $g_s$ .

- $A_\mu^a$  is now the gluon fields, and  $T^a$  is the matrices for the SU(3) gauge symmetry group.

- QCD contains more degrees of freedom due to this.

- The difference between U(1) and SU(2) is that the latter contains a more complex rotational symmetry.

- The field strength tensor becomes nonlinear due to the extra term.

## Comparing the strong force and QED

Electromagnetism or Quantum Electrodynamics(QED), a U(1) symmetry theory:

$$\mathcal{L}_{\text{QED}} = \sum_{f=\text{fermions}} \bar{\psi}_f (i\gamma^\mu (\partial_\mu + ieQ_f A_\mu) - m_f) \psi_f - \frac{1}{4} F_{\mu\nu} F^{\mu\nu}$$

Field strength tensor:

$$F_{\mu\nu} = \partial_\mu A_\nu - \partial_\nu A_\mu$$

The **strong nuclear force** or Quantum Chromo Dynamics(QCD), a SU(3) symmetry theory:

$$\mathcal{L}_{\text{QCD}} = \sum_{f=u,d,\dots} \bar{\psi}_f (i\gamma^\mu (\partial_\mu + ig_s A_\mu^a T^a) - m_f) \psi_f - \frac{1}{4} G_{\mu\nu}^a G^{a\mu\nu}$$

Field strength tensor:

$$G_{\mu\nu}^a = \partial_\mu A_\nu^a - \partial_\nu A_\mu^a - g_s f^{abc} A_\mu^b A_\nu^c$$

- QED is U(1) theory, and the simply means that it contains a simple rotational symmetry.

- $e$  is the coupling constant and  $Q_f$  is the charge.

- $\bar{\psi}_f$  and  $\psi_f$  are is the fermion fields.

- $A_\mu$  is the gauge fields.

- $\gamma^\mu$  is the Dirac matrices.

- First part contains the dynamics of all the fermions such as electrons, muons ect.

- Second part contains the dynamics of the photon fields in terms of the field strength tensor.

- Instead of a sum over all fermions, it is a sum over all quarks.

- The coupling constant is now the strong coupling,  $g_s$ .

- $A_\mu^a$  is now the gluon fields, and  $T^a$  is the matrices for the SU(3) gauge symmetry group.

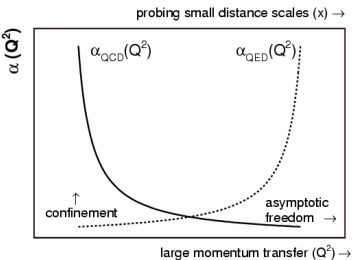
- QCD contains more degrees of freedom due to this.

- The difference between U(1) and SU(2) is that the latter contains a more complex rotational symmetry.

- The field strength tensor becomes nonlinear due to the extra term.

# Why is the strong force strong?

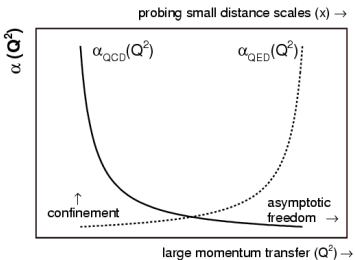
- Coupling constant  $\alpha$  is the strength of the force in an interaction.



- In physics, a **coupling constant** or gauge coupling parameter (or, more simply, a coupling), is a number that determines the strength of the force exerted in an interaction.

[https://www-cdf.fnal.gov/~group/WORK/DISSERTATION/diss\\_page.htm](https://www-cdf.fnal.gov/~group/WORK/DISSERTATION/diss_page.htm)

# Why is the strong force strong?

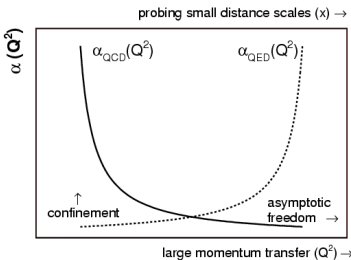


- Coupling constant  $\alpha$  is the strength of the force in an interaction.
- QED becomes stronger - QCD becomes weaker at higher energies.

- In physics, a **coupling constant** or gauge coupling parameter (or, more simply, a coupling), is a number that determines the strength of the force exerted in an interaction.
- We cannot make **perturbative expansions** in the low-energy regime of the strong nuclear force.

[https://www-cdf.fnal.gov/~group/WORK/DISSERTATION/diss\\_page.htm](https://www-cdf.fnal.gov/~group/WORK/DISSERTATION/diss_page.htm)

# Why is the strong force strong?

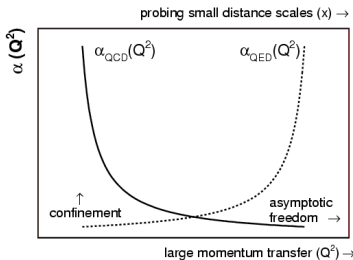


- Coupling constant  $\alpha$  is the strength of the force in an interaction.
- QED becomes stronger - QCD becomes weaker at higher energies.
- Can't use perturbation theory on strong force in low-energy regime!

- In physics, a **coupling constant** or gauge coupling parameter (or, more simply, a coupling), is a number that determines the strength of the force exerted in an interaction.
- We cannot make **perturbative expansions** in the low-energy regime of the strong nuclear force.

[https://www-cdf.fnal.gov/~group/WORK/DISSERTATION/diss\\_page.htm](https://www-cdf.fnal.gov/~group/WORK/DISSERTATION/diss_page.htm)

# Why is the strong force strong?

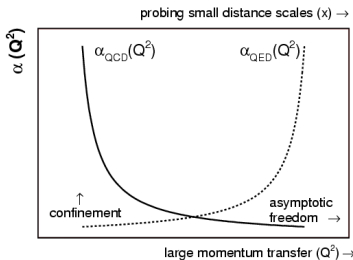


[https://www-cdf.fnal.gov/~group/WORK/DISSERTATION/diss\\_page.htm](https://www-cdf.fnal.gov/~group/WORK/DISSERTATION/diss_page.htm)

- Coupling constant  $\alpha$  is the strength of the force in an interaction.
- QED becomes stronger - QCD becomes weaker at higher energies.
- Can't use perturbation theory on strong force in low-energy regime!
- Need to understand the low-energy regime to understand phenomena such as **confinement**.

- In physics, a **coupling constant** or gauge coupling parameter (or, more simply, a coupling), is a number that determines the strength of the force exerted in an interaction.
- We cannot make **perturbative expansions** in the low-energy regime of the strong nuclear force.
- Which is really a shame, since many interesting phenomena such as **confinement** is a low-energy phenomena.

# Why is the strong force strong?



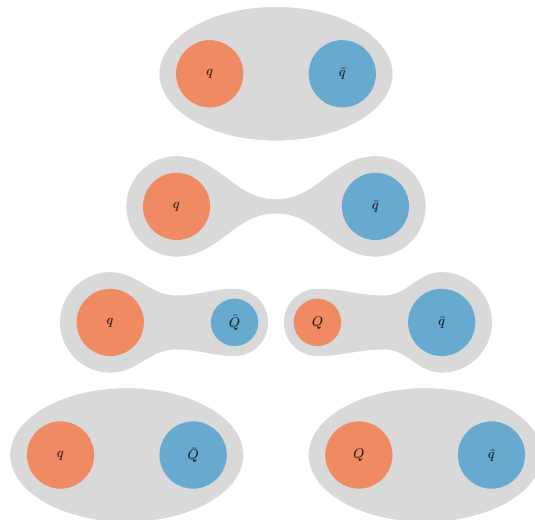
[https://www-cdf.fnal.gov/~group/WORK/DISSERTATION/diss\\_page.htm](https://www-cdf.fnal.gov/~group/WORK/DISSERTATION/diss_page.htm)

- Coupling constant  $\alpha$  is the strength of the force in an interaction.
- QED becomes stronger - QCD becomes weaker at higher energies.
- Can't use perturbation theory on strong force in low-energy regime!
- Need to understand the low-energy regime to understand phenomena such as **confinement**.

- In physics, a **coupling constant** or gauge coupling parameter (or, more simply, a coupling), is a number that determines the strength of the force exerted in an interaction.
- We cannot make **perturbative expansions** in the low-energy regime of the strong nuclear force.
- Which is really a shame, since many interesting phenomena such as **confinement** is a low-energy phenomena.

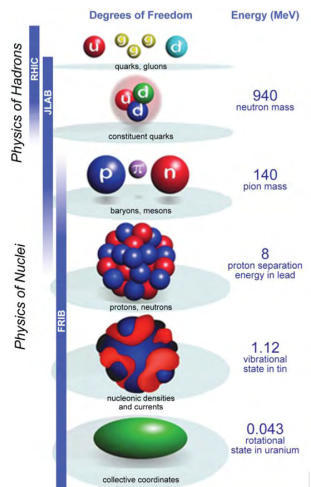
## Confinement: a low-energy phenomena

No free quarks in nature!



If we try to pull apart **two quarks in a meson**, more and more energy is required until we have enough energy to spontaneously create a **quark-antiquark pair**, forming thus **two new mesons**.

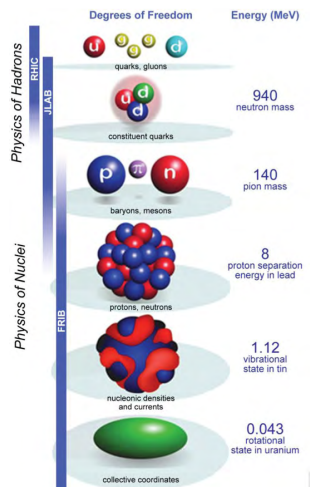
# QCD and nuclear physics



- Need to understand the low-energy regime in order to better understand nuclear physics!

The most fundamental theory we currently have of nuclear physics is QCD. Understanding QCD will help us understand nuclear physics and more *emergent* theories. But to bridge the gaps between these theories is difficult, as QCD contains a large number of degrees of freedom. Thus, a numerical approach is needed.

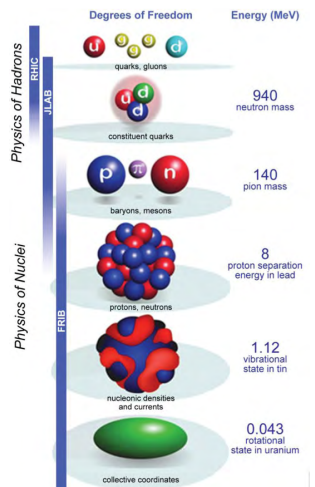
# QCD and nuclear physics



- Need to understand the low-energy regime in order to better understand nuclear physics!
- Want to bridge the gap between theories that operate at different scales.

The most fundamental theory we currently have of nuclear physics is QCD. Understanding QCD will help us understand nuclear physics and more *emergent* theories. But to bridge the gaps between these theories is difficult, as QCD contains a large number of degrees of freedom. Thus, a numerical approach is needed.

# QCD and nuclear physics



- Need to understand the low-energy regime in order to better understand nuclear physics!
- Want to bridge the gap between theories that operate at different scales.
- → numerical methods(e.g. lattice QCD)

The most fundamental theory we currently have of nuclear physics is QCD. Understanding QCD will help us understand nuclear physics and more *emergent* theories. But to bridge the gaps between these theories is difficult, as QCD contains a large number of degrees of freedom. Thus, a numerical approach is needed.

We currently have...

- A theory for QCD in the **continuum**.

We currently have...

- A theory for QCD in the **continuum**.
- Which we solve QCD by a Feynman **path integral**.

We currently have...

- A theory for QCD in the **continuum**.
- Which we solve QCD by a Feynman **path integral**.
- We want to solve this **numerically**.

We currently have...

- A theory for QCD in the **continuum**.
- Which we solve QCD by a Feynman **path integral**.
- We want to solve this **numerically**.
- → need to **discretize** the path integral.

We currently have...

- A theory for QCD in the **continuum**.
- Which we solve QCD by a Feynman **path integral**.
- We want to solve this **numerically**.
- → need to **discretize** the path integral.

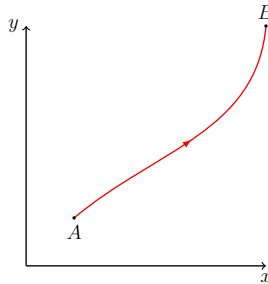
But first, we need to know *what* a path integral is.

## How we measure: path integrals

Going from  $t_0$  at  $A$  to a time  $t_1$  at  $B$  can be given in terms of a path integral.

## How we measure: path integrals

Going from  $t_0$  at  $A$  to a time  $t_1$  at  $B$  can be given in terms of a path integral.

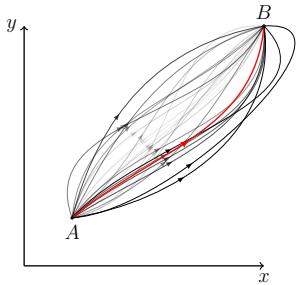


Classically, only one possible path obtained from the principle of least action.

- Classically we only have one available path given to us from the principle of least action.

## How we measure: path integrals

Going from  $t_0$  at  $A$  to a time  $t_1$  at  $B$  can be given in terms of a path integral.

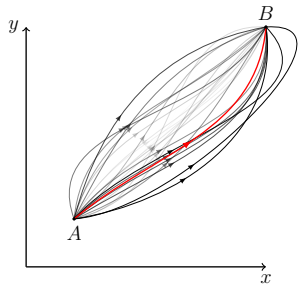


In quantum mechanics, there is lots of possible paths.

- Classically we only have one available path given to us from the principle of least action.
- In quantum mechanics, we have several available paths, which are all weighted by some probability amplitude.

## How we measure: path integrals

Going from  $t_0$  at  $A$  to a time  $t_1$  at  $B$  can be given in terms of a path integral.



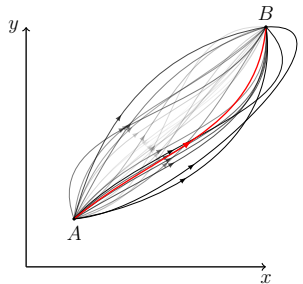
In quantum mechanics, there is lots of possible paths.

Principle of least action (or stationary condition):  $\frac{\delta}{\delta x(t)} (S [x(t)]) = 0$

- Classically we only have one available path given to us from the principle of least action.
- In quantum mechanics, we have several available paths, which are all weighted by some probability amplitude.

## How we measure: path integrals

Going from  $t_0$  at  $A$  to a time  $t_1$  at  $B$  can be given in terms of a path integral.



In quantum mechanics, there is lots of possible paths.

Principle of least action (or stationary condition):  $\frac{\delta}{\delta x(t)} (S [x(t)]) = 0$

Sum over all possible paths → the most likely path.

- Classically we only have one available path given to us from the principle of least action.
- In quantum mechanics, we have several available paths, which are all weighted by some probability amplitude.

## Path integrals

Given a field  $\phi_M$  in Minkowski space, the *partition function*  $Z$  is given by

$$Z = \int \mathcal{D}\phi_M e^{\frac{i}{\hbar} S_M[\phi_M]}$$

$\downarrow \quad \hbar = 1, \quad \tau \rightarrow -it$       imaginary time( $\rightarrow$  Euclidean space)!

$$= \int \mathcal{D}\phi e^{-S[\phi]}$$

where  $\mathcal{D}$  is an integration of all possible paths in space.

- We go to imaginary time in order to avoid oscillations due to the complex phase.
- We must also change the action  $S$ , so it is expressed in Euclidean space.
- We will **remain in Euclidean space** for the rest of the presentation.

## Path integrals

Given a field  $\phi_M$  in Minkowski space, the *partition function*  $Z$  is given by

$$Z = \int \mathcal{D}\phi_M e^{\frac{i}{\hbar} S_M[\phi_M]}$$

$\downarrow \quad \hbar = 1, \quad \tau \rightarrow -it \quad \text{imaginary time} (\rightarrow \text{Euclidean space})!$

$$= \int \mathcal{D}\phi e^{-S[\phi]}$$

where  $\mathcal{D}$  is an integration of all possible paths in space.

An observable  $O$  becomes,

$$\langle O \rangle = \frac{1}{Z} \int \mathcal{D}\phi O[\phi] e^{-S[\phi]}$$

with action given in terms of spacetime integral of the Lagrangian  $\mathcal{L}$

$$S = \int d^4x \mathcal{L}$$

- We go to imaginary time in order to avoid oscillations due to the complex phase.
- We must also change the action  $S$ , so it is expressed in Euclidean space.
- We will **remain in Euclidean space** for the rest of the presentation.
- Then, the expectation value given in terms to all possible paths with  $Z$  as a weight.

## Path integrals

Given a field  $\phi_M$  in Minkowski space, the *partition function*  $Z$  is given by

$$\begin{aligned} Z &= \int \mathcal{D}\phi_M e^{\frac{i}{\hbar} S_M[\phi_M]} \\ &\downarrow \quad \hbar = 1, \quad \tau \rightarrow -it \quad \text{imaginary time} (\rightarrow \text{Euclidean space})! \\ &= \int \mathcal{D}\phi e^{-S[\phi]} \end{aligned}$$

where  $\mathcal{D}$  is an integration of all possible paths in space.

An observable  $O$  becomes,

$$\langle O \rangle = \frac{1}{Z} \int \mathcal{D}\phi O[\phi] e^{-S[\phi]}$$

with action given in terms of spacetime integral of the Lagrangian  $\mathcal{L}$

$$S = \int d^4x \mathcal{L}$$

Difficult to calculate the all possible paths → discretize spacetime

- We go to imaginary time in order to avoid oscillations due to the complex phase.
- We must also change the action  $S$ , so it is expressed in Euclidean space.
- We will **remain in Euclidean space** for the rest of the presentation.
- Then, the expectation value given in terms to all possible paths with  $Z$  as a weight.
- It is difficult to calculate all of the possible paths, so instead we discretize spacetime with the field value at every spacetime point instead.

## Path integrals

Given a field  $\phi_M$  in Minkowski space, the *partition function*  $Z$  is given by

$$\begin{aligned} Z &= \int \mathcal{D}\phi_M e^{\frac{i}{\hbar} S_M[\phi_M]} \\ &\downarrow \quad \hbar = 1, \quad \tau \rightarrow -it \quad \text{imaginary time} (\rightarrow \text{Euclidean space})! \\ &= \int \mathcal{D}\phi e^{-S[\phi]} \end{aligned}$$

where  $\mathcal{D}$  is an integration of all possible paths in space.

An observable  $O$  becomes,

$$\langle O \rangle = \frac{1}{Z} \int \mathcal{D}\phi O[\phi] e^{-S[\phi]}$$

with action given in terms of spacetime integral of the Lagrangian  $\mathcal{L}$

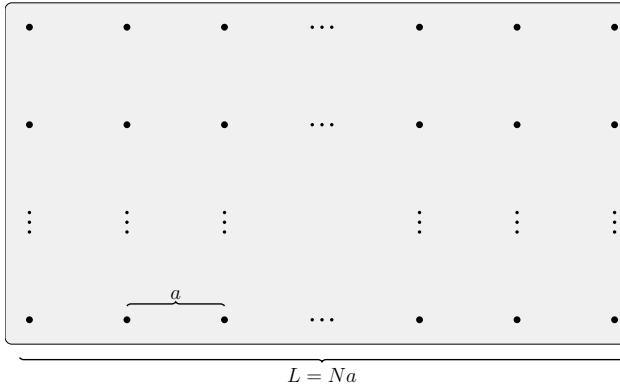
$$S = \int d^4x \mathcal{L}$$

Difficult to calculate the all possible paths → discretize spacetime

- We go to imaginary time in order to avoid oscillations due to the complex phase.
- We must also change the action  $S$ , so it is expressed in Euclidean space.
- We will **remain in Euclidean space** for the rest of the presentation.
- Then, the expectation value given in terms to all possible paths with  $Z$  as a weight.
- It is difficult to calculate all of the possible paths, so instead we discretize spacetime with the field value at every spacetime point instead.

## Discretizing the path integral

$N$  is the number of points on the lattice.



- We now have a integral over the field at every spacetime point.

Path integral integration measure becomes

$$\int \mathcal{D}\phi = \prod_{x_\mu} \int d\phi_{x_\mu}$$

- We now have a integral over the field at every spacetime point.

Path integral integration measure becomes

$$\int \mathcal{D}\phi = \prod_{x_\mu} \int d\phi_{x_\mu}$$

We integrate over each spacetime point.

## Discretizing the path integral

- We now have a integral over the field at every spacetime point.
- This poses another challenge, namely that we quickly have a large number of integrals. Say for a  $32^4$  lattice, we will have  $n^{2^{20}}$  integration points using conventional integration methods, i.e. the trapezoidal method.

Path integral integration measure becomes

$$\int \mathcal{D}\phi = \prod_{x_\mu} \int d\phi_{x_\mu}$$

We integrate over each spacetime point.

$32 \times 32 \times 32 \times 32 = 2^{20} \rightarrow n^{2^{20}}$  integration points.

## Discretizing the path integral

Path integral integration measure becomes

$$\int \mathcal{D}\phi = \prod_{x_\mu} \int d\phi_{x_\mu}$$

We integrate over each spacetime point.

$32 \times 32 \times 32 \times 32 = 2^{20} \rightarrow n^{2^{20}}$  integration points.

A **statistical approach** using importance sampling is needed for generating gauge configurations.

- We now have a integral over the field at every spacetime point.
- This poses another challenge, namely that we quickly have a large number of integrals. Say for a  $32^4$  lattice, we will have  $n^{2^{20}}$  integration points using conventional integration methods, i.e. the trapezoidal method.
- This require us to use statistical methods with some sort of importance sampling.

## Discretizing the path integral

Path integral integration measure becomes

$$\int \mathcal{D}\phi = \prod_{x_\mu} \int d\phi_{x_\mu}$$

We integrate over each spacetime point.

$32 \times 32 \times 32 \times 32 = 2^{20} \rightarrow n^{2^{20}}$  integration points.

A **statistical approach** using importance sampling is needed for generating gauge configurations.

- We now have a integral over the field at every spacetime point.
- This poses another challenge, namely that we quickly have a large number of integrals. Say for a  $32^4$  lattice, we will have  $n^{2^{20}}$  integration points using conventional integration methods, i.e. the trapezoidal method.
- This require us to use statistical methods with some sort of importance sampling.

The 2D Ising model is given by:

$$H = -J \sum_{\langle i,j \rangle} S_i S_j - h \sum_i S_i$$

The 2D Ising model is given by:

$$H = -J \sum_{\langle i,j \rangle} S_i S_j - h \sum_i S_i$$

- Ising model only has two possible values at a spin site  $S_i$ :  $\uparrow, \downarrow$

The 2D Ising model is given by:

$$H = -J \sum_{\langle i,j \rangle} S_i S_j - h \sum_i S_i$$

- Ising model only has two possible values at a spin site  $S_i$ :  $\uparrow, \downarrow$
- QCD many more degrees of freedom: quarks, gluons, color, charge, ...

The 2D Ising model is given by:

$$H = -J \sum_{\langle i,j \rangle} S_i S_j - h \sum_i S_i$$

- Ising model only has two possible values at a spin site  $S_i$ :  $\uparrow, \downarrow$
- QCD many more degrees of freedom: quarks, gluons, color, charge, ...
- With  $N = 10$ , a lattice in the Ising model has the size  $10 \times 10 = 100$ .

The 2D Ising model is given by:

$$H = -J \sum_{\langle i,j \rangle} S_i S_j - h \sum_i S_i$$

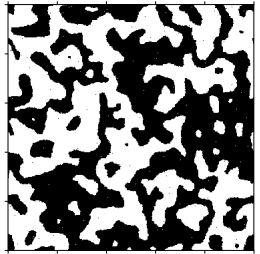
- Ising model only has two possible values at a spin site  $S_i$ :  $\uparrow, \downarrow$
- QCD many more degrees of freedom: quarks, gluons, color, charge, ...
- With  $N = 10$ , a lattice in the Ising model has the size  $10 \times 10 = 100$ .
- A lattice in LQCD is however  $N^4 = 10000$ .

Then what is a configuration?

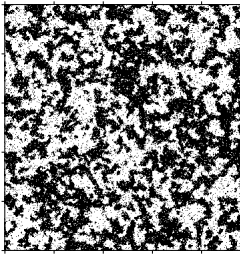
Two possible values indicated by either black or white dots.

Looking at a spin lattice of the Ising model,

$T = 1.10$



$T = 2.10$

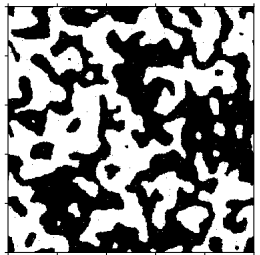


## Then what is a configuration?

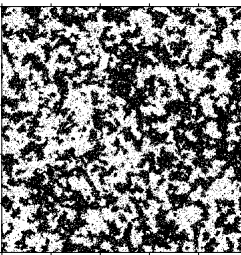
Two possible values indicated by either black or white dots.

Looking at a spin lattice of the Ising model,

$T = 1.10$



$T = 2.10$



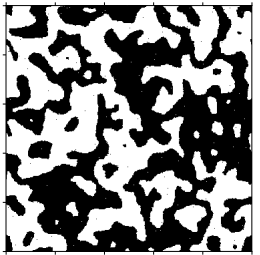
- A **configuration** in the Ising model is a given *arrangement of the spins*.

## Then what is a configuration?

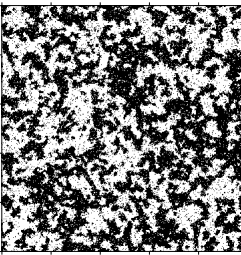
Two possible values indicated by either black or white dots.

Looking at a spin lattice of the Ising model,

$T = 1.10$



$T = 2.10$



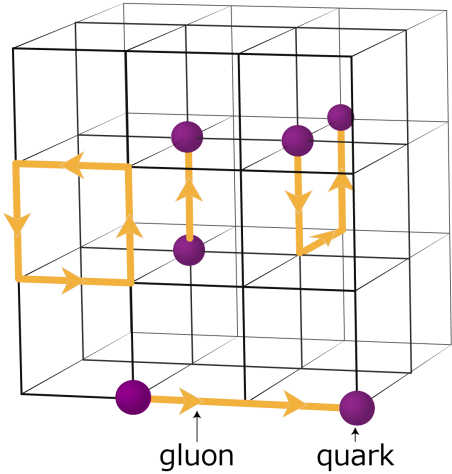
- A **configuration** in the Ising model is a given *arrangement of the spins*.
- A **configuration** in LQCD is a given *arrangement of the gauge field*.

An expectation value becomes

$$\langle O \rangle = \frac{1}{N_{\text{cfg}}} \sum_{i=1}^{N_{\text{cfg}}} O[\phi_i] + \mathcal{O}\left(\frac{1}{\sqrt{N_{\text{cfg}}}}\right)$$

where  $\phi_i$  is a generated gauge configuration(or just a general configuration).

# QCD on the lattice



- The lattice is a cube in 4D.
- Quarks at lattice, gluons in-between (**links**).
- Maintains the SU(3) symmetry by introducing links.
- Closed loops are gauge invariant.
- Smallest possible object: the plaquette.
- Paths of links with fermions as end points are gauge invariant.
- However, from now on we will ignore any fermions.

[http://www.jicfus.jp/en/wp-content/uploads/2012/12/  
LatticeQCD.png](http://www.jicfus.jp/en/wp-content/uploads/2012/12/LatticeQCD.png)

We exclude fermions to only look at the gauge fields,

$$S_G = \frac{1}{2} \int d^4x \text{tr} (G_{\mu\nu})^2$$

## Links

- *Links*  $U_\mu(n)$  tell us how the gauge field at lattice location  $n$  changes in a given direction  $\hat{\mu}$

## Links

- *Links*  $U_\mu(n)$  tell us how the gauge field at lattice location  $n$  changes in a given direction  $\hat{\mu}$
- Four links at every lattice site (one for each Lorentz index). Opposite direction given by its inverse.

- *Links*  $U_\mu(n)$  tell us how the gauge field at lattice location  $n$  changes in a given direction  $\hat{\mu}$
- Four links at every lattice site (one for each Lorentz index). Opposite direction given by its inverse.
- Links are complex  $3 \times 3$  matrices of the group SU(3) with properties of,

- *Links*  $U_\mu(n)$  tell us how the gauge field at lattice location  $n$  changes in a given direction  $\hat{\mu}$
- Four links at every lattice site(one for each Lorentz index). Opposite direction given by its inverse.
- Links are complex  $3 \times 3$  matrices of the group SU(3) with properties of,

$$U_\mu^\dagger(x) = U_\mu^{-1}(x), \quad \det(U_\mu(x)) = 1.$$

- *Links*  $U_\mu(n)$  tell us how the gauge field at lattice location  $n$  changes in a given direction  $\hat{\mu}$
- Four links at every lattice site (one for each Lorentz index). Opposite direction given by its inverse.
- Links are complex  $3 \times 3$  matrices of the group  $SU(3)$  with properties of,

$$U_\mu^\dagger(x) = U_\mu^{-1}(x), \quad \det(U_\mu(x)) = 1.$$

From this we can build a lattice action,

$$S_G[U] = \frac{\beta}{3} \sum_{n \in \Lambda} \sum_{\mu < \nu} \text{Re} \text{tr} [1 - U_\mu(n) U_\nu(n + \hat{\mu}) U_\mu(n + \hat{\nu})^\dagger U_\nu(n)^\dagger],$$

with  $\beta = 6/g_S^2$

Notice that in this expression we have that the four links that forms a *plaquette*, which is the smallest possible gauge invariant object, are dependent on the neighboring object at  $\hat{\mu}$  and  $\hat{\nu}$ .

- Links  $U_\mu(n)$  tell us how the gauge field at lattice location  $n$  changes in a given direction  $\hat{\mu}$
- Four links at every lattice site (one for each Lorentz index). Opposite direction given by its inverse.
- Links are complex  $3 \times 3$  matrices of the group SU(3) with properties of,

$$U_\mu^\dagger(x) = U_\mu^{-1}(x), \quad \det(U_\mu(x)) = 1.$$

From this we can build a lattice action,

$$S_G[U] = \frac{\beta}{3} \sum_{n \in \Lambda} \sum_{\mu < \nu} \text{Re} \text{tr} [1 - U_\mu(n) U_\nu(n + \hat{\mu}) U_\mu(n + \hat{\nu})^\dagger U_\nu(n)^\dagger],$$

with  $\beta = 6/g_S^2$

Notice that in this expression we have that the four links that forms a *plaquette*, which is the smallest possible gauge invariant object, are dependent on the neighboring object at  $\hat{\mu}$  and  $\hat{\nu}$ .

Since we are dealing with SU(3) matrices, we have that we in reality are performing pure matrix algebra. Due to the size of the lattice we would like to split this calculation.

- Links  $U_\mu(n)$  tell us how the gauge field at lattice location  $n$  changes in a given direction  $\hat{\mu}$
- Four links at every lattice site (one for each Lorentz index). Opposite direction given by its inverse.
- Links are complex  $3 \times 3$  matrices of the group SU(3) with properties of,

$$U_\mu^\dagger(x) = U_\mu^{-1}(x), \quad \det(U_\mu(x)) = 1.$$

From this we can build a lattice action,

$$S_G[U] = \frac{\beta}{3} \sum_{n \in \Lambda} \sum_{\mu < \nu} \text{Re} \text{tr} [1 - U_\mu(n) U_\nu(n + \hat{\mu}) U_\mu(n + \hat{\nu})^\dagger U_\nu(n)^\dagger],$$

with  $\beta = 6/g_S^2$

Notice that in this expression we have that the four links that forms a *plaquette*, which is the smallest possible gauge invariant object, are dependent on the neighboring object at  $\hat{\mu}$  and  $\hat{\nu}$ .

Since we are dealing with SU(3) matrices, we have that we in reality are performing pure matrix algebra. Due to the size of the lattice we would like to split this calculation.

## Parallelization: distributing the problem

Number of points in a lattice:

$$\underbrace{N^3}_{\text{Spatial}} \times \underbrace{N_T}_{\text{Temporal}} \times \underbrace{4}_{\text{Links}} \times \underbrace{9}_{\text{SU(3) matrix}} \times \underbrace{2}_{\mathbb{C}\text{-numbers}} = 72N^3N_T,$$

Number of points in a lattice:

$$\underbrace{N^3}_{\text{Spatial}} \times \underbrace{N_T}_{\text{Temporal}} \times \underbrace{4}_{\text{Links}} \times \underbrace{9}_{\text{SU(3) matrix}} \times \underbrace{2}_{\mathbb{C}\text{-numbers}} = 72N^3N_T,$$

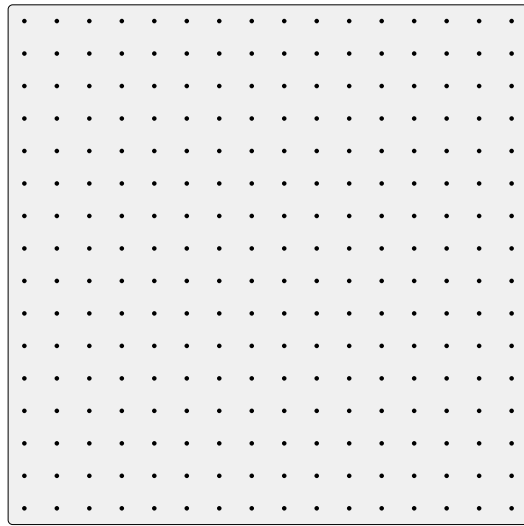
Too large to solve on any single computer.

Number of points in a lattice:

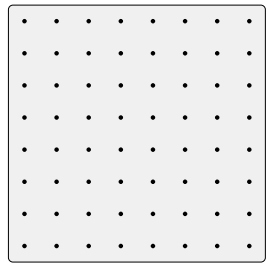
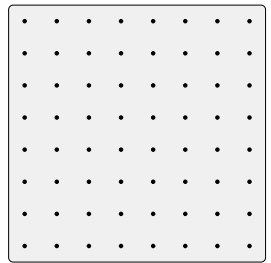
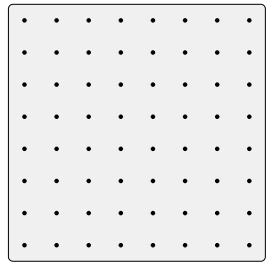
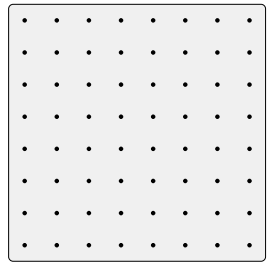
$$\underbrace{N^3}_{\text{Spatial}} \times \underbrace{N_T}_{\text{Temporal}} \times \underbrace{4}_{\text{Links}} \times \underbrace{9}_{\text{SU(3) matrix}} \times \underbrace{2}_{\mathbb{C}\text{-numbers}} = 72N^3N_T,$$

Too large to solve on any single computer.

## Parallelization: splitting the hypercube



## Parallelization: splitting the hypercube



## Parallelization: shifts

We need a message passing interface for communication(MPI).

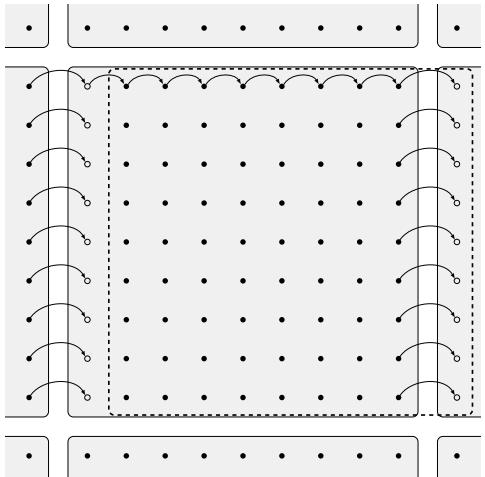
## Parallelization: shifts

We need a message passing interface for communication(MPI).

Implemented *shifts* for sharing data.

## Parallelization: shifts

We need a message passing interface for communication(MPI).  
Implemented *shifts* for sharing data.



So far, we have ...

- We calculate the action using links.

- a procedure for calculating the action using links.

## So far, we have ...

- a procedure for calculating the action using links.
- a statistical Monte Carlo method for solving the path integral.

- We calculate the action using links.
- We will use the Metropolis Monte Carlo method for solving the path integral and generating configurations.

## So far, we have ...

- a procedure for calculating the action using links.
- a statistical Monte Carlo method for solving the path integral.
- We have a method for parallelization for handling the computations.

- We calculate the action using links.
- We will use the Metropolis Monte Carlo method for solving the path integral and generating configurations.
- We have a method for handling the computations.

## So far, we have ...

- a procedure for calculating the action using links.
- a statistical Monte Carlo method for solving the path integral.
- We have a method for parallelization for handling the computations.

However, some observable are problematic...

- We calculate the action using links.
- We will use the Metropolis Monte Carlo method for solving the path integral and generating configurations.
- We have a method for handling the computations.
- However, some observables are problematic, and we need to apply some method of renormalization in order to retrieve sensible results..

## So far, we have ...

- a procedure for calculating the action using links.
- a statistical Monte Carlo method for solving the path integral.
- We have a method for parallelization for handling the computations.

However, some observable are problematic...

- We calculate the action using links.
- We will use the Metropolis Monte Carlo method for solving the path integral and generating configurations.
- We have a method for handling the computations.
- However, some observables are problematic, and we need to apply some method of renormalization in order to retrieve sensible results..

$$\partial_{t_f} B_\mu(x, t_f) = D_\nu G_{\nu\mu}(x, t_f)$$

$$B_\mu(x, t_f) \Big|_{t_f=0} = A_\mu(x)$$

- Solves this by integrating along  $t_f$  called *flow time*<sup>1</sup>

---

<sup>1</sup>Lüscher [2010]

$$\partial_{t_f} B_\mu(x, t_f) = D_\nu G_{\nu\mu}(x, t_f)$$

$$B_\mu(x, t_f)|_{t_f=0} = A_\mu(x)$$

- Solves this by integrating along  $t_f$  called *flow time*<sup>1</sup>
- $B_\mu(x, t_f)$  is the gauge field  $A_\mu(x)$  at a flow time  $t_f$ .

---

<sup>1</sup>Lüscher [2010]

$$\partial_{t_f} B_\mu(x, t_f) = D_\nu G_{\nu\mu}(x, t_f)$$

$$B_\mu(x, t_f) \Big|_{t_f=0} = A_\mu(x)$$

- Solves this by integrating along  $t_f$  called *flow time*<sup>1</sup>
- $B_\mu(x, t_f)$  is the gauge field  $A_\mu(x)$  at a flow time  $t_f$ .
- $D_\nu = \partial_\nu + [B_\mu(x, t_f), \cdot]$

---

<sup>1</sup>Lüscher [2010]

$$\partial_{t_f} B_\mu(x, t_f) = D_\nu G_{\nu\mu}(x, t_f)$$

$$B_\mu(x, t_f)|_{t_f=0} = A_\mu(x)$$

- Solves this by integrating along  $t_f$  called *flow time*<sup>1</sup>
- $B_\mu(x, t_f)$  is the gauge field  $A_\mu(x)$  at a flow time  $t_f$ .
- $D_\nu = \partial_\nu + [B_\mu(x, t_f), \cdot]$
- Field strength tensor:

$$G_{\mu\nu}(x, t_f) = \partial_\mu B_\nu(x, t_f) - \partial_\nu B_\mu(x, t_f) - i[B_\mu(x, t_f), B_\nu(x, t_f)]$$

---

<sup>1</sup>Lüscher [2010]

$$\partial_{t_f} B_\mu(x, t_f) = D_\nu G_{\nu\mu}(x, t_f)$$

$$B_\mu(x, t_f)|_{t_f=0} = A_\mu(x)$$

- Solves this by integrating along  $t_f$  called *flow time*<sup>1</sup>
- $B_\mu(x, t_f)$  is the gauge field  $A_\mu(x)$  at a flow time  $t_f$ .
- $D_\nu = \partial_\nu + [B_\mu(x, t_f), \cdot]$
- Field strength tensor:

$$G_{\mu\nu}(x, t_f) = \partial_\mu B_\nu(x, t_f) - \partial_\nu B_\mu(x, t_f) - i[B_\mu(x, t_f), B_\nu(x, t_f)]$$

An analogy: the diffusion equation:

$$\frac{\partial}{\partial t_f} B_\mu(x, t_f) \approx \partial_x^2 B_\mu(x, t_f)$$

---

<sup>1</sup>Lüscher [2010]

- The gauge field at  $t_f > 0$  is a **smooth, renormalized field**.

- The gauge field at  $t_f > 0$  is a **smooth, renormalized field**.
- Allows us to measure certain quantities such as the **topological charge**,  $Q$

- The gauge field at  $t_f > 0$  is a **smooth, renormalized field**.
- Allows us to measure certain quantities such as the **topological charge**,  $Q$



## Results

---

## Ensembles

Points in lattice given by  $N^3 \times N_T$ .

Ensemble	$\beta = 6/g_S^2$	$N$	$N_T$	$N_{\text{cfg}}$	$a$ [fm]	Config. size[GB]
$A$	6.0	24	48	1000	0.0931(4)	0.356
$B$	6.1	28	56	1000	0.0791(3)	0.659
$C$	6.2	32	64	2000	0.0679(3)	1.125
$D_1$	6.45	32	32	1000	0.0478(3)	0.563
$D_2$	6.45	48	96	250	0.0478(3)	5.695

- I implemented the methods discussed under a code I call GLAC, and will now present some of the results I generated using this code.
- The main ensembles made for this thesis.
- An ensemble is a collection of configurations using similar size and lattice spacing.
- Notice that the size of a lattice is 16 times larger when doubling the dimensions.
- **Ensemble  $D_2$  only has 250 configurations.**
  - Every configuration was flown with  $N_{\text{flow}} = 1000$  flow steps.
  - Since there are so few data configurations, resampling techniques such as bootstrapping were implemented.

## Ensembles

Points in lattice given by  $N^3 \times N_T$ .

Ensemble	$\beta = 6/g_S^2$	$N$	$N_T$	$N_{\text{cfg}}$	$a$ [fm]	Config. size[GB]
$A$	6.0	24	48	1000	0.0931(4)	0.356
$B$	6.1	28	56	1000	0.0791(3)	0.659
$C$	6.2	32	64	2000	0.0679(3)	1.125
$D_1$	6.45	32	32	1000	0.0478(3)	0.563
$D_2$	6.45	48	96	250	0.0478(3)	5.695

A scale  $t_0$  was set using the energy and gradient flow.

- I implemented the methods discussed under a code I call GLAC, and will now present some of the results I generated using this code.
- The main ensembles made for this thesis.
- An ensemble is a collection of configurations using similar size and lattice spacing.
- Notice that the size of a lattice is 16 times larger when doubling the dimensions.
- **Ensemble  $D_2$  only has 250 configurations.**
  - Every configuration was flown with  $N_{\text{flow}} = 1000$  flow steps.
  - Since there are so few data configurations, resampling techniques such as bootstrapping were implemented.
  - A scale  $t_0$  was set, in which more details exist in the backup slides.

## Ensembles

Points in lattice given by  $N^3 \times N_T$ .

Ensemble	$\beta = 6/g_S^2$	$N$	$N_T$	$N_{\text{cfg}}$	$a$ [fm]	Config. size[GB]
$A$	6.0	24	48	1000	0.0931(4)	0.356
$B$	6.1	28	56	1000	0.0791(3)	0.659
$C$	6.2	32	64	2000	0.0679(3)	1.125
$D_1$	6.45	32	32	1000	0.0478(3)	0.563
$D_2$	6.45	48	96	250	0.0478(3)	5.695

A scale  $t_0$  was set using the energy and gradient flow.

- I implemented the methods discussed under a code I call GLAC, and will now present some of the results I generated using this code.
- The main ensembles made for this thesis.
- An ensemble is a collection of configurations using similar size and lattice spacing.
- Notice that the size of a lattice is 16 times larger when doubling the dimensions.
- **Ensemble  $D_2$  only has 250 configurations.**
  - Every configuration was flown with  $N_{\text{flow}} = 1000$  flow steps.
  - Since there are so few data configurations, resampling techniques such as bootstrapping were implemented.
  - A scale  $t_0$  was set, in which more details exist in the backup slides.

## Topological charge

- QCD vacua(i.e. gauge fields) can be classified by their topological properties.

## Topological charge

- QCD vacua(i.e. gauge fields) can be classified by their topological properties.
- In this vacua, **instantons** are local minima of the Yang-Mills action in Euclidean space, as they are solutions to the e.o.m.

- **Instantons** can be viewed as local minima to the Yang-Mills action in Euclidean space, as they are localized solutions to the classical finite action equations of motion in Euclidean space.

## Topological charge

- QCD vacua(i.e. gauge fields) can be classified by their topological properties.
- In this vacua, **instantons** are local minima of the Yang-Mills action in Euclidean space, as they are solutions to the e.o.m.
- **Topological charge**  $Q$  can be viewed as a “measure” of instantons.

- **Instantons** can be viewed as local minima to the Yang-Mills action in Euclidean space, as they are localized solutions to the classical finite action equations of motion in Euclidean space.
- Instantons are significant in LQCD because of *critical slowing down* which we will return to later.

## Topological charge

- QCD vacua(i.e. gauge fields) can be classified by their topological properties.
- In this vacua, **instantons** are local minima of the Yang-Mills action in Euclidean space, as they are solutions to the e.o.m.
- **Topological charge**  $Q$  can be viewed as a “measure” of instantons.

$$Q = a^4 \sum_{n \in \Lambda} q(n),$$

with the charge density given by

$$q(n) = \frac{1}{32\pi^2} \epsilon_{\mu\nu\rho\sigma} \text{tr} [G_{\mu\nu}(n) G_{\rho\sigma}(n)].$$

- **Instantons** can be viewed as local minima to the Yang-Mills action in Euclidean space, as they are localized solutions to the classical finite action equations of motion in Euclidean space.
- Instantons are significant in LQCD because of *critical slowing down* which we will return to later.
- The charge is a **sum over the local charge** at every point in the gauge field.
- Can in a very crude manner be viewed as the “curl” of the gauge fields due to the Levi-Civita tensor.
- The **expectation value of  $Q$  is zero** due to it being **parity odd**.

## Topological charge

- QCD vacua(i.e. gauge fields) can be classified by their topological properties.
- In this vacua, **instantons** are local minima of the Yang-Mills action in Euclidean space, as they are solutions to the e.o.m.
- **Topological charge**  $Q$  can be viewed as a “measure” of instantons.

$$Q = a^4 \sum_{n \in \Lambda} q(n),$$

with the charge density given by

$$q(n) = \frac{1}{32\pi^2} \epsilon_{\mu\nu\rho\sigma} \text{tr} [G_{\mu\nu}(n) G_{\rho\sigma}(n)].$$

Integer valued and equally probably to have negative charge as positive,

$$\langle Q \rangle = 0$$

- **Instantons** can be viewed as local minima to the Yang-Mills action in Euclidean space, as they are localized solutions to the classical finite action equations of motion in Euclidean space.
- Instantons are significant in LQCD because of *critical slowing down* which we will return to later.
- The charge is a **sum over the local charge** at every point in the gauge field.
- Can in a very crude manner be viewed as the “curl” of the gauge fields due to the Levi-Civita tensor.
- The **expectation value of  $Q$  is zero** due to it being **parity odd**.
- The charge is integer valued.

## Topological charge

- QCD vacua(i.e. gauge fields) can be classified by their topological properties.
- In this vacua, **instantons** are local minima of the Yang-Mills action in Euclidean space, as they are solutions to the e.o.m.
- **Topological charge**  $Q$  can be viewed as a “measure” of instantons.

$$Q = a^4 \sum_{n \in \Lambda} q(n),$$

with the charge density given by

$$q(n) = \frac{1}{32\pi^2} \epsilon_{\mu\nu\rho\sigma} \text{tr} [G_{\mu\nu}(n) G_{\rho\sigma}(n)].$$

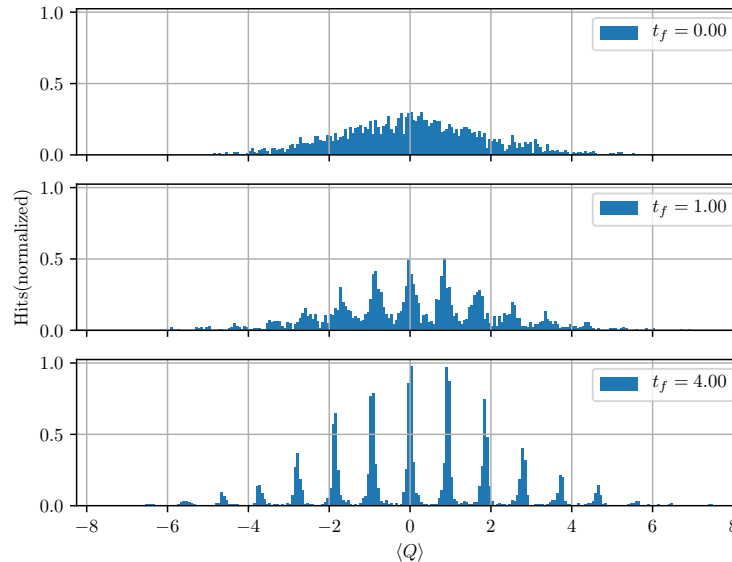
Integer valued and equally probably to have negative charge as positive,

$$\langle Q \rangle = 0$$

- **Instantons** can be viewed as local minima to the Yang-Mills action in Euclidean space, as they are localized solutions to the classical finite action equations of motion in Euclidean space.
- Instantons are significant in LQCD because of *critical slowing down* which we will return to later.
- The charge is a **sum over the local charge** at every point in the gauge field.
- Can in a very crude manner be viewed as the “curl” of the gauge fields due to the Levi-Civita tensor.
- The **expectation value of  $Q$  is zero** due to it being **parity odd**.
- The charge is integer valued.

## Topological charge distribution

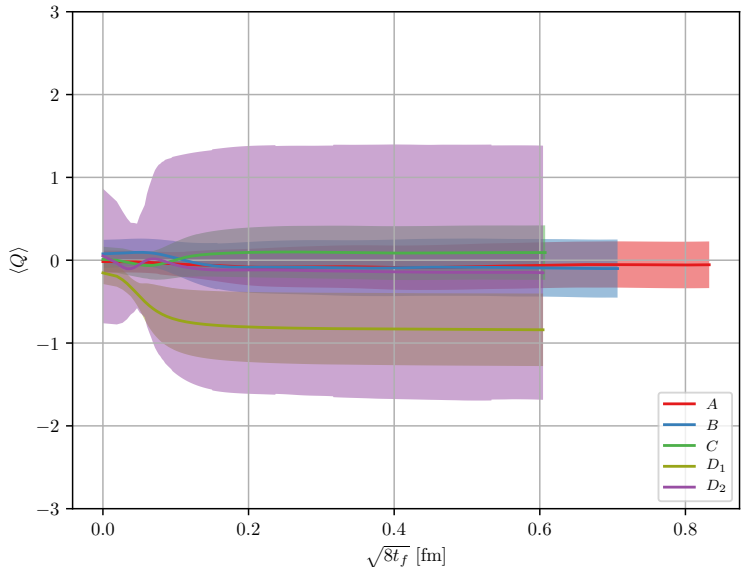
Histograms for the  $Q$  for ensemble  $G$  with a lattice of size  $N^3 \times N_T = 16^3 \times 32$  with  $\beta = 6.1$ , taken at different flow times  $t_f/a^2 = 0.0, 1.0, 4.0$  fm.



# Topological charge

*Animation created using LatViz.*

## Topological charge for our main ensembles



## Autocorrelations

- Why is the charge not centered around zero for certain ensembles?

- Charge around zero for ensemble  $C$ , but not as evident for ensemble  $D_2$ .
- Points clearly dependent on the previous point in  $D_2$ .

## Autocorrelations

- Why is the charge not centered around zero for certain ensembles?
- Let us look at the **autocorrelation** - the measure for correlations between gauge configurations in Monte Carlo time.
- Charge around zero for ensemble  $C$ , but not as evident for ensemble  $D_2$ .
- Points clearly dependent on the previous point in  $D_2$ .

## Autocorrelations

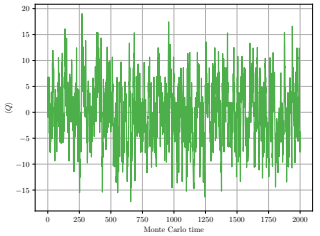
- Why is the charge not centered around zero for certain ensembles?
- Let us look at the **autocorrelation** - the measure for correlations between gauge configurations in Monte Carlo time.
- The autocorrelation is given as  $\Gamma(t) = \langle (x_i - \bar{x})(x_{i+t} - \bar{x}) \rangle$  and  $\tau_{\text{int}} = \frac{1}{2} + \sum_{t=1}^{\infty} \frac{\Gamma(t)}{\Gamma(0)}$ .
- Charge around zero for ensemble  $C$ , but not as evident for ensemble  $D_2$ .
- Points clearly dependent on the previous point in  $D_2$ .

## Autocorrelations

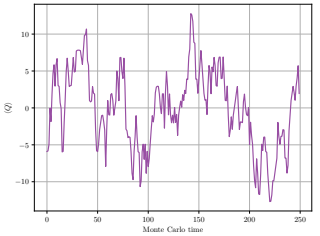
- Why is the charge not centered around zero for certain ensembles?
- Let us look at the **autocorrelation** - the measure for correlations between gauge configurations in Monte Carlo time.
- The autocorrelation is given as  $\Gamma(t) = \langle (x_i - x)(x_{i+t} - x) \rangle$  and  $\tau_{\text{int}} = \frac{1}{2} + \sum_{t=1}^{\infty} \frac{\Gamma(t)}{\Gamma(0)}$ .
- **Zero autocorrelation** corresponds to  $\tau_{\text{int}} = 0.5$
- Charge around zero for ensemble  $C$ , but not as evident for ensemble  $D_2$ .
- Points clearly dependent on the previous point in  $D_2$ .

## Autocorrelations

- Why is the charge not centered around zero for certain ensembles?
- Let us look at the **autocorrelation** - the measure for correlations between gauge configurations in Monte Carlo time.
- The autocorrelation is given as  $\Gamma(t) = \langle (x_i - \bar{x})(x_{i+t} - \bar{x}) \rangle$  and  $\tau_{\text{int}} = \frac{1}{2} + \sum_{t=1}^{\infty} \frac{\Gamma(t)}{\Gamma(0)}$ .
- **Zero autocorrelation** corresponds to  $\tau_{\text{int}} = 0.5$



Ensemble  $C$ ,  $32^3 \times 64$ ,  $\beta = 6.2$

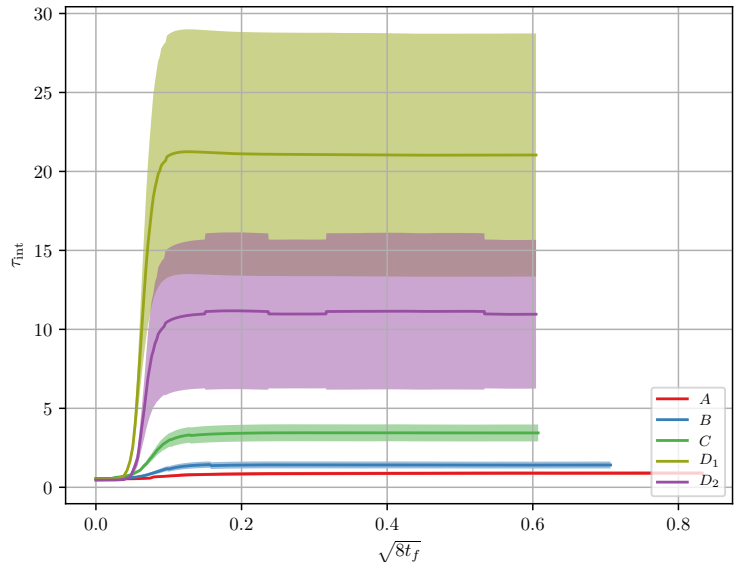


Ensemble  $D_2$ ,  $48^3 \times 96$ ,  $\beta = 6.45$

- Charge around zero for ensemble  $C$ , but not as evident for ensemble  $D_2$ .
- Points clearly dependent on the previous point in  $D_2$ .

## Topological charge autocorrelation

- The integrated autocorrelation  $\tau_{\text{int}}$  for topological charge for the five main ensembles.



## Critical slowing down

- Critical slowing down is the phenomena where we as the lattice spacing  $a$  decreases the required energy to tunnel from one topological sector to another increase.

## Critical slowing down

- Critical slowing down is the phenomena where we as the lattice spacing  $a$  decreases the required energy to tunnel from one topological sector to another increase.
- In the continuum, going from one topological sector, a region with similar topological charge, to another require infinite energy. As  $a \rightarrow 0$ , the amount of effort required to change the configuration increases.
- That is, going from one instanton sector to another requires many more updates and becomes an inherent problem in all LQCD calculations.

## Critical slowing down

- Critical slowing down is the phenomena where we as the lattice spacing  $a$  decreases the required energy to tunnel from one topological sector to another increase.
- In the continuum, going from one topological sector, a region with similar topological charge, to another require infinite energy. As  $a \rightarrow 0$ , the amount of effort required to change the configuration increases.
- → many more lattice updates are required in order to have independent gauge configurations.
- That is, going from one instanton sector to another requires many more updates and becomes an inherent problem in all LQCD calculations.
- In the continuum it would require an **infinite amount of energy** to go from **one instanton sector to another**. Thus as we  $a$  approaches the continuum, the amount of **effort**(number of updates etc.) required to generate **independent** gauge configurations **increases**.

## Critical slowing down

- Critical slowing down is the phenomena where we as the lattice spacing  $a$  decreases the required energy to tunnel from one topological sector to another increase.
- In the continuum, going from one topological sector, a region with similar topological charge, to another require infinite energy. As  $a \rightarrow 0$ , the amount of effort required to change the configuration increases.
- → many more lattice updates are required in order to have independent gauge configurations.
- That is, going from one instanton sector to another requires many more updates and becomes an inherent problem in all LQCD calculations.
- In the continuum it would require an **infinite amount of energy** to go from **one instanton sector to another**. Thus as we  $a$  approaches the continuum, the amount of **effort**(number of updates etc.) required to generate **independent** gauge configurations **increases**.

## Topological susceptibility

The *topological susceptibility* is given by

$$\chi_{\text{top}}^{1/4} = \frac{1}{V^{1/4}} \langle Q^2 \rangle^{1/4}$$

with  $V$  being the lattice volume and  $\langle Q^2 \rangle$  is the second momenta of the charge.

## Topological susceptibility

- R.h.s. is full QCD and l.h.s is from pure gauge theory.

The *topological susceptibility* is given by

$$\chi_{\text{top}}^{1/4} = \frac{1}{V^{1/4}} \langle Q^2 \rangle^{1/4}$$

with  $V$  being the lattice volume and  $\langle Q^2 \rangle$  is the second momenta of the charge.

The *Witten-Veneziano relation* is given by

$$m_{\eta'}^2 = \frac{2N_f}{f_\pi^2} \chi_{\text{top}}$$

## Topological susceptibility

The *topological susceptibility* is given by

$$\chi_{\text{top}}^{1/4} = \frac{1}{V^{1/4}} \langle Q^2 \rangle^{1/4}$$

with  $V$  being the lattice volume and  $\langle Q^2 \rangle$  is the second momenta of the charge.

The *Witten-Veneziano relation* is given by

$$m_{\eta'}^2 = \frac{2N_f}{f_\pi^2} \chi_{\text{top}}$$

with

- R.h.s. is full QCD and l.h.s is from pure gauge theory.
- We can use the Witten-Veneziano formula in order to extract an estimate for  $N_f$  using the topological susceptibility.

- pion decay constant  $f_\pi = 0.130(5)/\sqrt{2}$  GeV.

## Topological susceptibility

The *topological susceptibility* is given by

$$\chi_{\text{top}}^{1/4} = \frac{1}{V^{1/4}} \langle Q^2 \rangle^{1/4}$$

with  $V$  being the lattice volume and  $\langle Q^2 \rangle$  is the second momenta of the charge.

The *Witten-Veneziano relation* is given by

$$m_{\eta'}^2 = \frac{2N_f}{f_\pi^2} \chi_{\text{top}}$$

with

- pion decay constant  $f_\pi = 0.130(5)/\sqrt{2}$  GeV.
- $\eta'$  meson mass  $m_{\eta'} = 0.95778(6)$  GeV.

- R.h.s. is full QCD and l.h.s is from pure gauge theory.
- We can use the Witten-Veneziano formula in order to extract an estimate for  $N_f$  using the topological susceptibility.

## Topological susceptibility

The *topological susceptibility* is given by

$$\chi_{\text{top}}^{1/4} = \frac{1}{V^{1/4}} \langle Q^2 \rangle^{1/4}$$

with  $V$  being the lattice volume and  $\langle Q^2 \rangle$  is the second momenta of the charge.

The *Witten-Veneziano relation* is given by

$$m_{\eta'}^2 = \frac{2N_f}{f_\pi^2} \chi_{\text{top}}$$

with

- pion decay constant  $f_\pi = 0.130(5)/\sqrt{2}$  GeV.
- $\eta'$  meson mass  $m_{\eta'} = 0.95778(6)$  GeV.
- $N_f$  is the number of flavors(i.e. quark species involved in  $\eta'$ ).

- R.h.s. is full QCD and l.h.s is from pure gauge theory.
- We can use the Witten-Veneziano formula in order to extract an estimate for  $N_f$  using the topological susceptibility.

## Topological susceptibility

The *topological susceptibility* is given by

$$\chi_{\text{top}}^{1/4} = \frac{1}{V^{1/4}} \langle Q^2 \rangle^{1/4}$$

with  $V$  being the lattice volume and  $\langle Q^2 \rangle$  is the second momenta of the charge.

The *Witten-Veneziano relation* is given by

$$m_{\eta'}^2 = \frac{2N_f}{f_\pi^2} \chi_{\text{top}}$$

with

- pion decay constant  $f_\pi = 0.130(5)/\sqrt{2}$  GeV.
- $\eta'$  meson mass  $m_{\eta'} = 0.95778(6)$  GeV.
- $N_f$  is the number of flavors(i.e. quark species involved in  $\eta'$ ).

We expect  $N_f = 3$ .

- R.h.s. is full QCD and l.h.s is from pure gauge theory.
- We can use the Witten-Veneziano formula in order to extract an estimate for  $N_f$  using the topological susceptibility.
- This can help us understand the "quality" of the ensemble, as we would expect to be around  $N_f = 3$ .

## Topological susceptibility

The *topological susceptibility* is given by

$$\chi_{\text{top}}^{1/4} = \frac{1}{V^{1/4}} \langle Q^2 \rangle^{1/4}$$

with  $V$  being the lattice volume and  $\langle Q^2 \rangle$  is the second momenta of the charge.

The *Witten-Veneziano relation* is given by

$$m_{\eta'}^2 = \frac{2N_f}{f_\pi^2} \chi_{\text{top}}$$

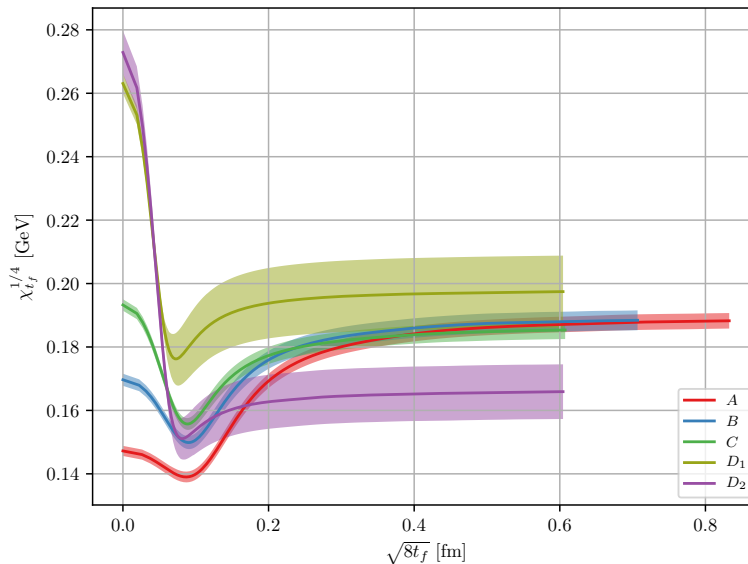
with

- pion decay constant  $f_\pi = 0.130(5)/\sqrt{2}$  GeV.
- $\eta'$  meson mass  $m_{\eta'} = 0.95778(6)$  GeV.
- $N_f$  is the number of flavors(i.e. quark species involved in  $\eta'$ ).

We expect  $N_f = 3$ .

- R.h.s. is full QCD and l.h.s is from pure gauge theory.
- We can use the Witten-Veneziano formula in order to extract an estimate for  $N_f$  using the topological susceptibility.
- This can help us understand the "quality" of the ensemble, as we would expect to be around  $N_f = 3$ .

## Topological susceptibility



- The topological susceptibility  $\chi_{tf}^{1/4}$  of the **main ensembles**.
- We have a **UV divergence at zeroth flow time**, hence to need for gradient flow which renormalizes this quantity.
- **Bootstrapped**  $N_{\text{bs}} = 500$  times.
- Corrected for autocorrelations with  $\sigma = \sqrt{2\tau_{\text{int}}}\sigma_0$ .

Ensembles	$\chi_{tf}^{1/4} (\langle Q^2 \rangle) [\text{GeV}]$	$N_f$	$\chi^2/\text{d.o.f}$
$A, B, C, D_2$	0.179(10)	3.75(29)	2.38
$A, B, C, D_1$	0.186(6)	3.21(25)	0.83
$A, B, C$	0.184(6)	3.37(26)	0.33

## The fourth cumulant

- Highly unstable, as we shall see.
- Will provide insight into the goodness of our ensembles.
- An  $R$ -value away from 1 will indicate that QCD cannot be described by the dilute instanton gas model.

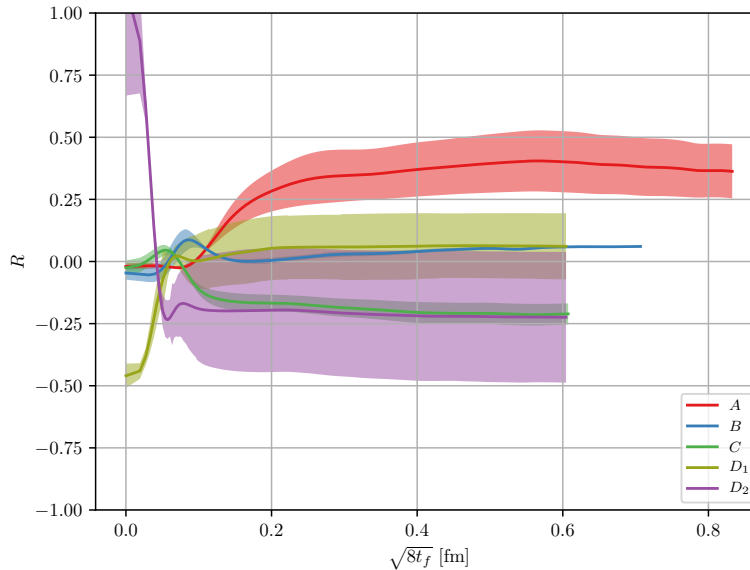
$$\langle Q^4 \rangle_c = \frac{1}{V^2} \left( \langle Q^4 \rangle - 3 \langle Q^2 \rangle^2 \right).$$

From this, we can also measure the ratio  $R$ ,

$$R = \frac{\langle Q^4 \rangle_c}{\frac{1}{V} \langle Q^2 \rangle} = \frac{1}{V} \frac{\langle Q^4 \rangle - 3 \langle Q^2 \rangle^2}{\langle Q^2 \rangle},$$

## The fourth cumulant

- The fourth cumulant ratio  $R = \langle Q^4 \rangle_C / \langle Q^2 \rangle$ .
- The results was analyzed using  $N_{\text{bs}} = 500$  bootstrap samples, with the error corrected for by  $\sqrt{2\tau_{\text{int}}}$ .



## The fourth cumulant at reference flow times

The fourth cumulant is taken at their individual reference scales seen in the third column. The data were analyzed with using a bootstrap analysis of  $N_{bs} = 500$  samples, with error corrected by the integrated autocorrelation,  $\sqrt{2\tau_{\text{int}}}$ .

Ensemble	$L/a$	$t_0/a^2$	$\langle Q^2 \rangle$	$\langle Q^4 \rangle$	$\langle Q^4 \rangle_C$	$R$
$A$	2.24	3.20(3)	0.78(4)	2.13(27)	0.282(67)	0.359(65)
$B$	2.21	4.43(4)	0.81(5)	1.98(23)	0.036(11)	0.044(11)
$C$	2.17	6.01(6)	0.77(4)	1.6(2)	-0.174(40)	-0.226(64)
$D_1$	1.53	12.2(1)	1.00(20)	3.01(1.07)	0.03(12)	0.03(12)
$D_2$	2.29	12.2(1)	0.497(100)	0.64(20)	-0.103(95)	-0.21(23)

## Comparing fourth cumulant

We can compare with article by Cè et al. [2015]

## Comparing fourth cumulant

- Parameters of the ensembles presented by Cè et al. [2015]. The first column is the ensemble name from the article. The letter indicates the volume, while the subindex indicates the  $\beta$  value. Ensembles of similar letters keep approximately the same length  $L$ .

Ensemble	$\beta$	$L/a$	$L$ [fm]	$a$ [fm]	$t_0/a^2$	$t_0/r_0^2$	$N_{\text{cfg}}$
$F_1$	5.96	16	1.632	0.102	2.7887(2)	0.1113(9)	1 440 000
$B_2$	6.05	14	1.218	0.087	3.7960(12)	0.1114(9)	144 000
$\tilde{D}_2$		17	1.479		3.7825(8)	0.1110(9)	
$B_3$	6.13	16	1.232	0.077	4.8855(15)	0.1113(10)	144 000
$\tilde{D}_3$		19	1.463		4.8722(11)	0.1110(10)	
$B_4$	6.21	18	1.224	0.068	6.2191(20)	0.1115(11)	144 000
$\tilde{D}_4$		21	1.428		6.1957(14)	0.1111(11)	

## Comparing fourth cumulant

Article	Thesis	Ratio( $\langle Q^2 \rangle$ )	Ratio( $\langle Q^4 \rangle$ )	Ratio( $\langle Q^4 \rangle_C$ )	Ratio( $R$ )
$F_1$	$A$	1.08(6)	1.34(18)	19.03(5.81)	17.64(4.48)
$B_2$	$A$	1.02(5)	1.15(15)	3.60(1.09)	3.54(90)
	$B$	1.04(6)	1.06(11)	0.480(74)	0.46(4)
$\tilde{D}_2$	$A$	1.02(5)	1.19(15)	8.31(1.99)	8.15(1.56)
	$B$	1.05(6)	1.10(12)	1.1(1)	1.06(3)
$B_3$	$B$	1.06(6)	1.10(12)	0.550(86)	0.52(5)
$\tilde{D}_3$	$B$	1.05(6)	1.11(12)	1.51(23)	1.4(1)
$B_4$	$C$	0.99(5)	0.86(8)	-2.32(46)	-2.35(59)
$\tilde{D}_4$	$C$	0.98(5)	0.85(8)	-3.95(96)	-4.05(1.19)

- A comparison between the results obtained in this thesis on the fourth cumulant, and by those similar in volume form Cè et al. [2015]. *Ratio* indicates that we are dividing our results by the ones in previous table. **1 is perfect overlap.**

## Comparing fourth cumulant

Article	Thesis	Ratio( $\langle Q^2 \rangle$ )	Ratio( $\langle Q^4 \rangle$ )	Ratio( $\langle Q^4 \rangle_C$ )	Ratio( $R$ )
$F_1$	$A$	1.08(6)	1.34(18)	19.03(5.81)	17.64(4.48)
$B_2$	$A$	1.02(5)	1.15(15)	3.60(1.09)	3.54(90)
	$B$	1.04(6)	1.06(11)	0.480(74)	0.46(4)
$\tilde{D}_2$	$A$	1.02(5)	1.19(15)	8.31(1.99)	8.15(1.56)
	$B$	1.05(6)	1.10(12)	1.1(1)	1.06(3)
$B_3$	$B$	1.06(6)	1.10(12)	0.550(86)	0.52(5)
$\tilde{D}_3$	$B$	1.05(6)	1.11(12)	1.51(23)	1.4(1)
$B_4$	$C$	0.99(5)	0.86(8)	-2.32(46)	-2.35(59)
$\tilde{D}_4$	$C$	0.98(5)	0.85(8)	-3.95(96)	-4.05(1.19)

- A comparison between the results obtained in this thesis on the fourth cumulant, and by those similar in volume form Cè et al. [2015]. *Ratio* indicates that we are dividing our results by the ones in previous table. **1 is perfect overlap.**

## The topological charge correlator and the effective glueball mass

- In pure Yang-Mills gauge theory, the states are stable.
- We will be looking at the state involving topological charge.

### The topological charge correlator

$$C(n_t) = \langle q(n_t)q(0) \rangle ,$$

is the correlator between two topological charge densities in Euclidean time.

## The topological charge correlator and the effective glueball mass

- In pure Yang-Mills gauge theory, the states are stable.
- We will be looking at the state involving topological charge.

### The topological charge correlator

$$C(n_t) = \langle q(n_t)q(0) \rangle,$$

is the correlator between two topological charge densities in Euclidean time.

The ground state in the correlator is given as

$$C(n_t) = A_0 e^{-n_t E_0} + A_1 e^{-n_t E_1} + \dots$$

## The topological charge correlator and the effective glueball mass

- In pure Yang-Mills gauge theory, the states are stable.
- We will be looking at the state involving topological charge.

### The topological charge correlator

$$C(n_t) = \langle q(n_t)q(0) \rangle,$$

is the correlator between two topological charge densities in Euclidean time.

The ground state in the correlator is given as

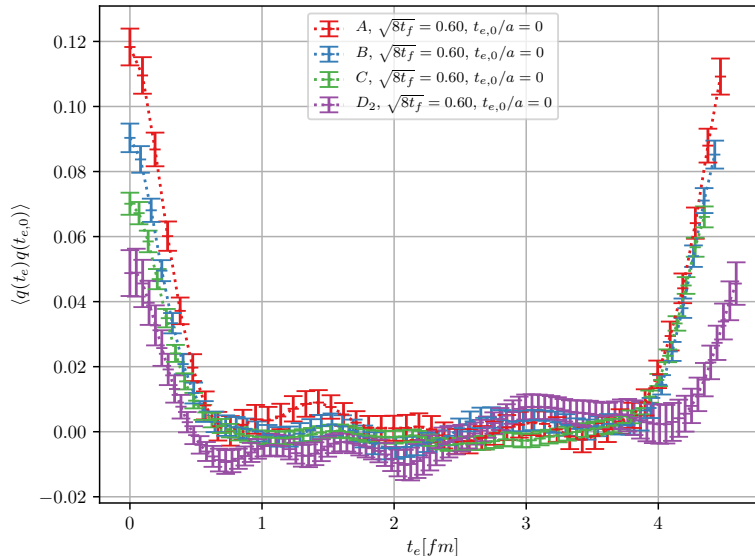
$$C(n_t) = A_0 e^{-n_t E_0} + A_1 e^{-n_t E_1} + \dots$$

from which the **effective glueball mass** can be extracted as

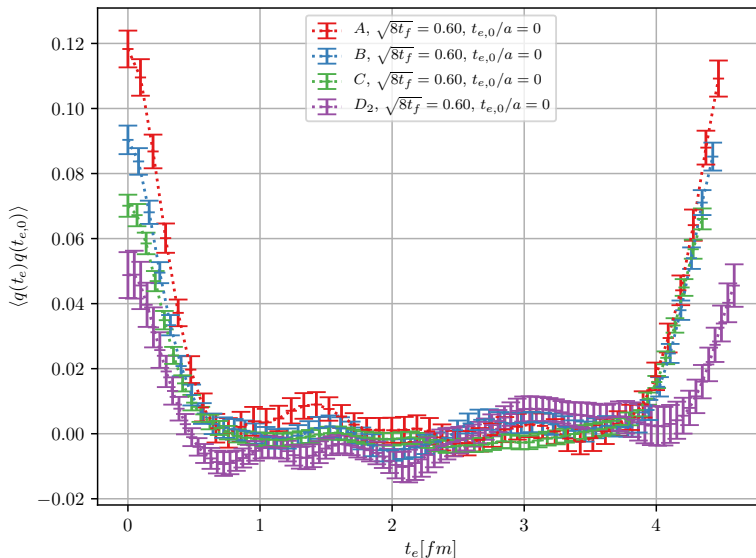
$$am_{\text{eff}} = \log \left( \frac{C(n_t)}{C(n_t + 1)} \right),$$

## The topological charge correlator

- The topological charge correlator for all of the ensembles except  $D_1$ . The  $x$ -axis contains the sink-source separation, as the source  $q(0)$  is placed at  $t_e = 0$  fm, and the sink  $q(t_e)$  is taken at  $t_e$ .

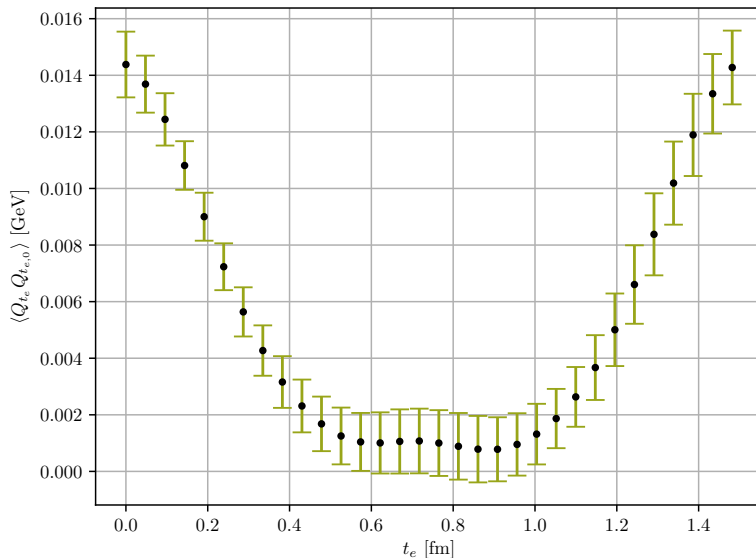


## The topological charge correlator



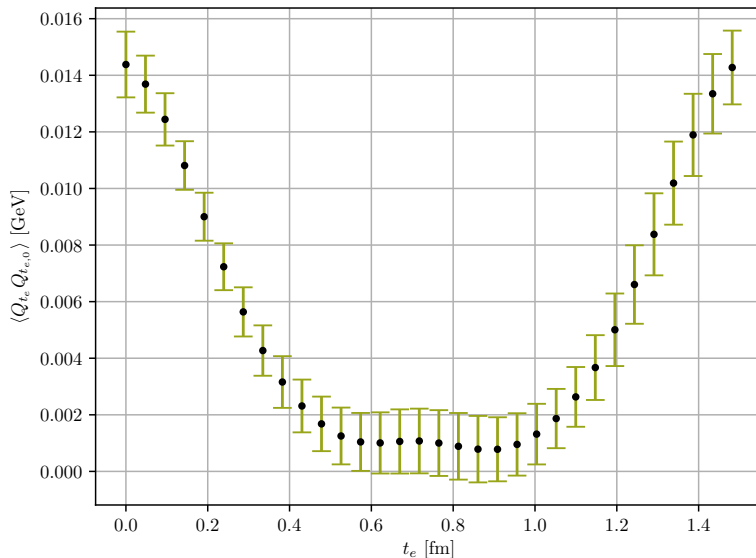
- The topological charge correlator for all of the ensembles except  $D_1$ . The  $x$ -axis contains the sink-source separation, as the source  $q(0)$  is placed at  $t_e = 0$  fm, and the sink  $q(t_e)$  is taken at  $t_e$ .
- We since the ensembles are of different lattice sizes, we plot th  $D_1$  separately.

## The topological charge correlator



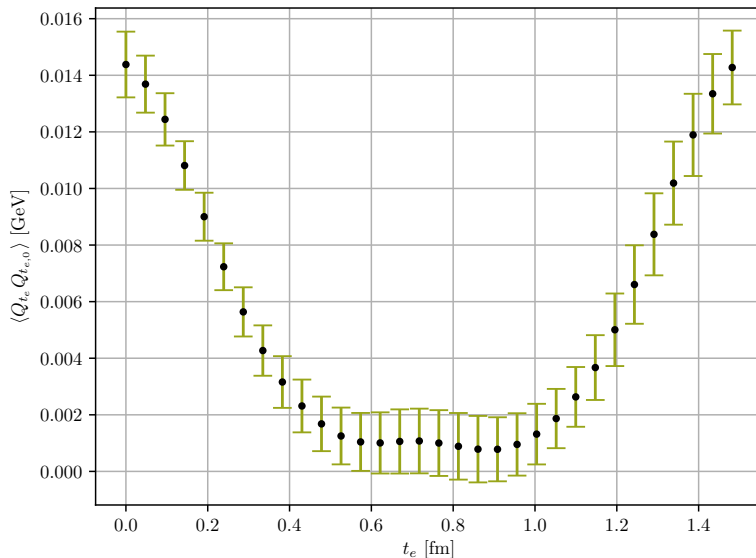
- The topological charge correlator for all of the ensembles except  $D_1$ . The  $x$ -axis contains the sink-source separation, as the source  $q(0)$  is placed at  $t_e = 0$  fm, and the sink  $q(t_e)$  is taken at  $t_e$ .
- We since the ensembles are of different lattice sizes, we plot th  $D_1$  separately.
- The topological charge correlator for the  $D_1$ . The source  $q(0)$  is placed at  $t_e = 0$  fm and the sink  $q(t_e)$  is taken at  $t_e$ .

## The topological charge correlator



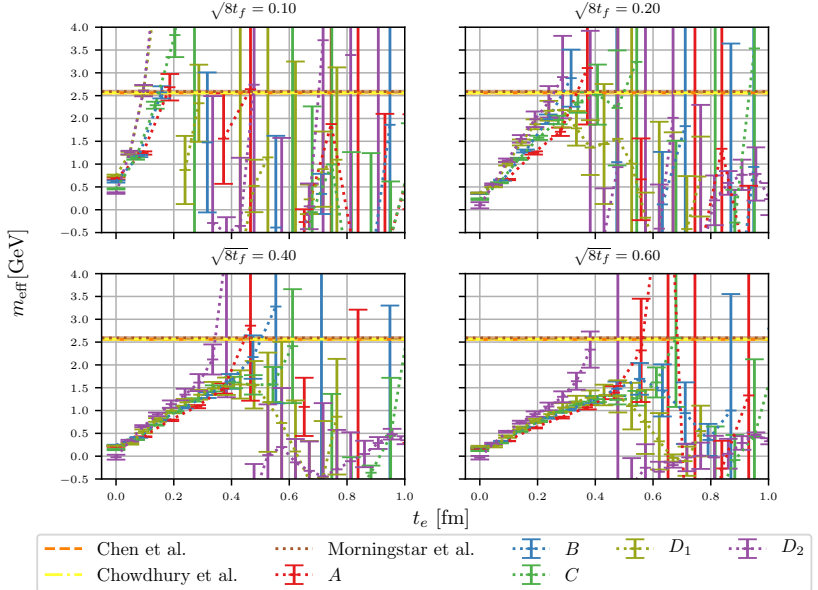
- The topological charge correlator for all of the ensembles except  $D_1$ . The  $x$ -axis contains the sink-source separation, as the source  $q(0)$  is placed at  $t_e = 0$  fm, and the sink  $q(t_e)$  is taken at  $t_e$ .
- We since the ensembles are of different lattice sizes, we plot th  $D_1$  separately.
- The topological charge correlator for the  $D_1$ . The source  $q(0)$  is placed at  $t_e = 0$  fm and the sink  $q(t_e)$  is taken at  $t_e$ .
- We would expect an **exponential dampening**.

## The topological charge correlator



- The topological charge correlator for all of the ensembles except  $D_1$ . The  $x$ -axis contains the sink-source separation, as the source  $q(0)$  is placed at  $t_e = 0$  fm, and the sink  $q(t_e)$  is taken at  $t_e$ .
- We since the ensembles are of different lattice sizes, we plot th  $D_1$  separately.
- The topological charge correlator for the  $D_1$ . The source  $q(0)$  is placed at  $t_e = 0$  fm and the sink  $q(t_e)$  is taken at  $t_e$ .
- We would expect an **exponential dampening**.

# The effective glueball mass



Conclusion, future developments  
and final thoughts

---

## Conclusion

- Created a code (GLAC) capable of generating and flowing gauge configurations.
- Checked scaling and parameter optimization.

## Conclusion

- Created a code (GLAC) capable of generating and flowing gauge configurations.
  - Verified to match other code bases down to machine precision.
- Checked scaling and parameter optimization.
- Same results as Chroma down to machine precision.

## Conclusion

- Created a code (GLAC) capable of generating and flowing gauge configurations.
  - Verified to match other code bases down to machine precision.
- Created a code (LatViz) for visualizing gauge fields.

- Checked scaling and parameter optimization.
- Same results as Chroma down to machine precision.

## Conclusion

- Created a code (GLAC) capable of generating and flowing gauge configurations.
  - Verified to match other code bases down to machine precision.
- Created a code (LatViz) for visualizing gauge fields.
- $\langle Q \rangle \neq 0$  for some ensembles → understood with autocorrelation.
- Checked scaling and parameter optimization.
- Same results as Chroma down to machine precision.
- $\langle Q \rangle$

## Conclusion

- Created a code (GLAC) capable of generating and flowing gauge configurations.
  - Verified to match other code bases down to machine precision.
- Created a code (LatViz) for visualizing gauge fields.
- $\langle Q \rangle \neq 0$  for some ensembles → understood with autocorrelation.
- The topological susceptibility  $\chi_f^{1/4}$  and  $N_f$
- Checked scaling and parameter optimization.
- Same results as Chroma down to machine precision.
- $\langle Q \rangle$
- $\chi_f^{1/4}$ . Matches well with other papers

## Conclusion

- Created a code (GLAC) capable of generating and flowing gauge configurations.
  - Verified to match other code bases down to machine precision.
- Created a code (LatViz) for visualizing gauge fields.
- $\langle Q \rangle \neq 0$  for some ensembles → understood with autocorrelation.
- The topological susceptibility  $\chi_f^{1/4}$  and  $N_f$
- $\langle Q^4 \rangle_C$  and  $R$ . Sensitive quantities - need large statistics.
- Checked scaling and parameter optimization.
- Same results as Chroma down to machine precision.
- $\langle Q \rangle$
- $\chi_f^{1/4}$ . Matches well with other papers
- $\langle Q^4 \rangle_C$  and  $R$ . Sensitive quantity, matches well of first and second moment.

## Conclusion

- Created a code (GLAC) capable of generating and flowing gauge configurations.
  - Verified to match other code bases down to machine precision.
- Created a code (LatViz) for visualizing gauge fields.
- $\langle Q \rangle \neq 0$  for some ensembles → understood with autocorrelation.
- The topological susceptibility  $\chi_f^{1/4}$  and  $N_f$
- $\langle Q^4 \rangle_C$  and  $R$ . Sensitive quantities - need large statistics.
- Topological charge correlator  $\langle q(n_t)q(0) \rangle$  and glueball mass.
- Checked scaling and parameter optimization.
- Same results as Chroma down to machine precision.
- $\langle Q \rangle$
- $\chi_f^{1/4}$ . Matches well with other papers
- $\langle Q^4 \rangle_C$  and  $R$ . Sensitive quantity, matches well of first and second moment.
- Topological charge correlator  $\langle q(n_t)q(0) \rangle$  and glueball mass.

## Conclusion

- Created a code (GLAC) capable of generating and flowing gauge configurations.
  - Verified to match other code bases down to machine precision.
- Created a code (LatViz) for visualizing gauge fields.
- $\langle Q \rangle \neq 0$  for some ensembles → understood with autocorrelation.
- The topological susceptibility  $\chi_f^{1/4}$  and  $N_f$
- $\langle Q^4 \rangle_C$  and  $R$ . Sensitive quantities - need large statistics.
- Topological charge correlator  $\langle q(n_t)q(0) \rangle$  and glueball mass.
- Statistics, autocorrelation and critical slowing down.

- Checked scaling and parameter optimization.
- Same results as Chroma down to machine precision.
- $\langle Q \rangle$
- $\chi_f^{1/4}$ . Matches well with other papers
- $\langle Q^4 \rangle_C$  and  $R$ . Sensitive quantity, matches well of first and second moment.
- Topological charge correlator  $\langle q(n_t)q(0) \rangle$  and glueball mass.
- Critical slowing down, which makes transitioning to a new, independent configuration difficult. This inhibits the gathering of statistics, and helps us explain why we for larger  $\beta$  values have fewer independent gauge configurations.

## Conclusion

- Created a code (GLAC) capable of generating and flowing gauge configurations.
  - Verified to match other code bases down to machine precision.
- Created a code (LatViz) for visualizing gauge fields.
- $\langle Q \rangle \neq 0$  for some ensembles → understood with autocorrelation.
- The topological susceptibility  $\chi_f^{1/4}$  and  $N_f$
- $\langle Q^4 \rangle_C$  and  $R$ . Sensitive quantities - need large statistics.
- Topological charge correlator  $\langle q(n_t)q(0) \rangle$  and glueball mass.
- Statistics, autocorrelation and critical slowing down.
- The energy, the scale  $t_0$  and  $w_0$  were also calculated match what is found in the literature, i.e. Lüscher [2010] and Cè et al. [2015].

- Checked scaling and parameter optimization.
- Same results as Chroma down to machine precision.
- $\langle Q \rangle$
- $\chi_f^{1/4}$ . Matches well with other papers
- $\langle Q^4 \rangle_C$  and  $R$ . Sensitive quantity, matches well of first and second moment.
- Topological charge correlator  $\langle q(n_t)q(0) \rangle$  and glueball mass.
- Critical slowing down, which makes transitioning to a new, independent configuration difficult. This inhibits the gathering of statistics, and helps us explain why we for larger  $\beta$  values have fewer independent gauge configurations.

- Better statistics - more gauge configurations.

- Better statistics - more gauge configurations.
- Implement better actions with operators that have smaller error contributions.

- Better statistics - more gauge configurations.
- Implement better actions with operators that have smaller error contributions.
- Fermions and HMC(Hybrid Monte Carlo).

Thank you for listening.

Questions?

## References

---

S. Borsanyi, S. Durr, Z. Fodor, C. Hoelbling, S. D. Katz, S. Krieg, T. Kurth, L. Lellouch, T. Lippert, C. McNeile, and K. K. Szabo. High-precision scale setting in lattice QCD. *Journal of High Energy Physics*, 2012(9), September 2012. ISSN 1029-8479. doi: [10.1007/JHEP09\(2012\)010](https://doi.org/10.1007/JHEP09(2012)010). URL <http://arxiv.org/abs/1203.4469>. arXiv: 1203.4469.

Marco Cè, Cristian Consonni, Georg P. Engel, and Leonardo Giusti. Non-Gaussianities in the topological charge distribution of the SU(3) Yang–Mills theory. *Physical Review D*, 92(7), October 2015. ISSN 1550-7998, 1550-2368. doi: [10.1103/PhysRevD.92.074502](https://doi.org/10.1103/PhysRevD.92.074502). URL <http://arxiv.org/abs/1506.06052>. arXiv: 1506.06052.

Martin Lüscher. Properties and uses of the Wilson flow in lattice QCD. *Journal of High Energy Physics*, 2010(8), August 2010. ISSN 1029-8479. doi: [10.1007/JHEP08\(2010\)071](https://doi.org/10.1007/JHEP08(2010)071). URL <http://arxiv.org/abs/1006.4518>. arXiv: 1006.4518.

Hans Munthe-Kaas. Runge–Kutta methods on Lie groups. *BIT Numerical Mathematics*, 38(1):92–111, March 1998. ISSN 0006-3835, 1572-9125. doi: [10.1007/BF02510919](https://doi.org/10.1007/BF02510919). URL <http://link.springer.com/10.1007/BF02510919>.

## Extra slides

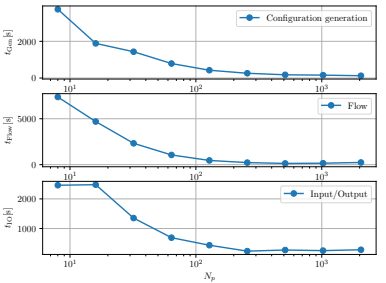
---

# Scaling

- Strong scaling

We checked three types of scaling,

- Strong scaling: *fixed problem* and a variable  $N_p$  cores

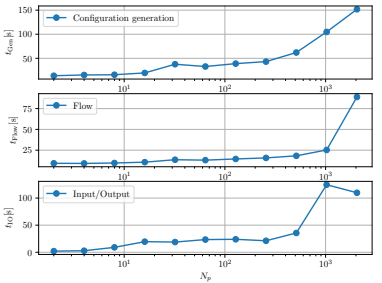


# Scaling

We checked three types of scaling,

- Strong scaling
- Weak scaling

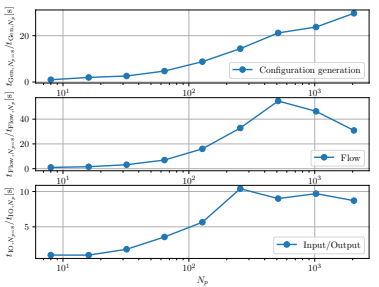
- **Strong scaling:** *fixed problem and a variable  $N_p$  cores*
- **Weak scaling:** *fixed problem per processor and a variable  $N_p$  cores.*



# Scaling

We checked three types of scaling,

- **Strong scaling:** *fixed problem and a variable  $N_p$  cores*
- **Weak scaling:** *fixed problem per processor and a variable  $N_p$  cores.*
- **Speedup:** defined as  $S(p) = \frac{t_{N_p}}{t_{N_p,0}}$ .



- Strong scaling
- Weak scaling
- The speedup of the configuration generation, flowing, and IO. The speedup is calculated by dividing the run time of each  $N_p$  run, with the run time of the run with the least number of processors,  $N_p = 8$ .

We checked three types of scaling,

- Strong scaling
- Weak scaling
- The speedup of the configuration generation, flowing, and IO. The speedup is calculated by dividing the run time of each  $N_p$  run, with the run time of the run with the least number of processors,  $N_p = 8$ .
- The IO was optimized later to be a factor of ten or more faster.

- **Strong scaling:** *fixed problem and a variable  $N_p$  cores*
- **Weak scaling:** *fixed problem per processor and a variable  $N_p$  cores.*
- **Speedup:** defined as  $S(p) = \frac{t_{N_p}}{t_{N_p,0}}$ .

We checked three types of scaling,

- **Strong scaling:** *fixed problem and a variable  $N_p$  cores*
- **Weak scaling:** *fixed problem per processor and a variable  $N_p$  cores.*
- **Speedup:** defined as  $S(p) = \frac{t_{N_p}}{t_{N_p,0}}$ .

We appear to have a plateau around 512 cores.

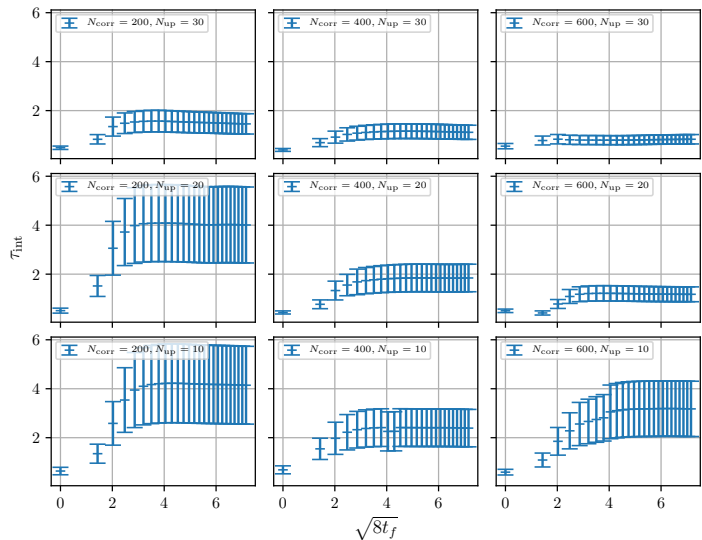
- Strong scaling
- Weak scaling
- The speedup of the configuration generation, flowing, and IO. The speedup is calculated by dividing the run time of each  $N_p$  run, with the run time of the run with the least number of processors,  $N_p = 8$ .
- The IO was optimized later to be a factor of ten or more faster.

## Optimizing the gauge configuration generation

- We run for different values for  $N_{\text{up}}$  and  $N_{\text{corr}}$  to see what gives optimizes **computational cost** and **autocorrelation**.
- The integrated autocorrelation time for topological charge  $\langle Q \rangle$  for a lattice of size  $N = 16$  and  $N_T = 32$  with  $\beta = 6.0$  for combinations of  $N_{\text{corr}} \in [200, 400, 600]$  and  $N_{\text{up}} \in [10, 20, 30]$ , plotted against flow time  $\sqrt{8t_f}$ .

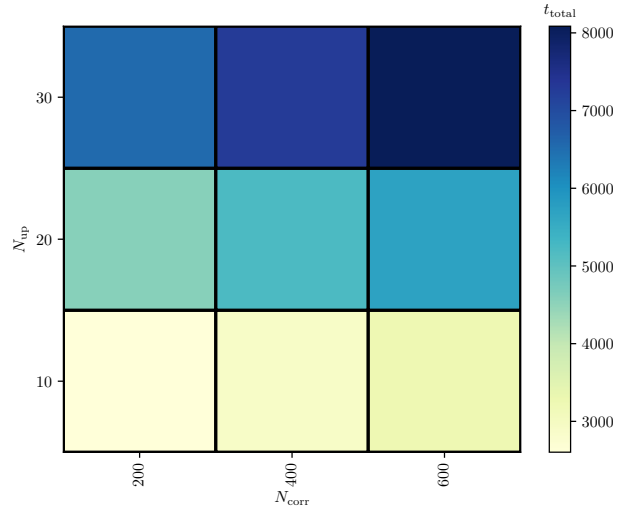
Generated 200 configurations for a lattice of size  $N^3 \times N_T = 16^3 \times 32$  and  $\beta = 6.0$ , for combinations of  $N_{\text{corr}} \in [200, 400, 600]$  and  $N_{\text{up}} \in [10, 20, 30]$ .

# Optimizing the gauge configuration generation



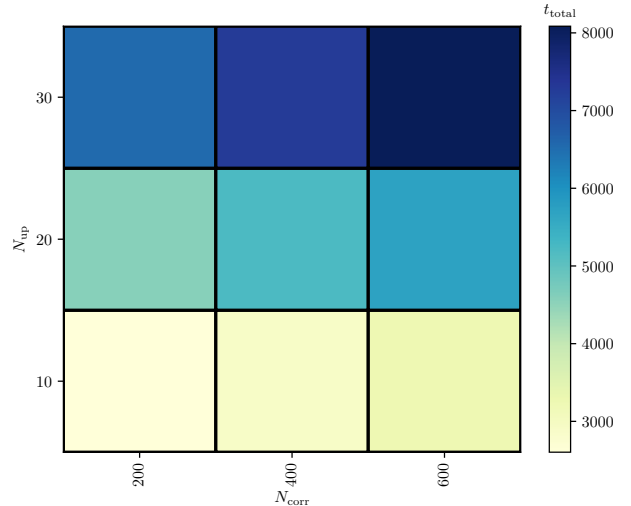
- We run for different values for  $N_{up}$  and  $N_{corr}$  to see what gives optimizes **computational cost** and **autocorrelation**.
- The integrated autocorrelation time for topological charge  $\langle Q \rangle$  for a lattice of size  $N = 16$  and  $N_T = 32$  with  $\beta = 6.0$  for combinations of  $N_{corr} \in [200, 400, 600]$  and  $N_{up} \in [10, 20, 30]$ , plotted against flow time  $\sqrt{8t_f}$ .
- The time taking to generate 200 configurations and flowing them  $N_{flow} = 250$  flow steps for a lattice of size  $N = 16$  and  $N_T = 32$ , with  $\beta = 6.0$  for combinations of  $N_{corr} \in [200, 400, 600]$  and  $N_{up} \in [10, 20, 30]$ .

## Optimizing the gauge configuration generation



- We run for different values for  $N_{\text{up}}$  and  $N_{\text{corr}}$  to see what gives optimizes **computational cost** and **autocorrelation**.
- The integrated autocorrelation time for topological charge  $\langle Q \rangle$  for a lattice of size  $N = 16$  and  $N_T = 32$  with  $\beta = 6.0$  for combinations of  $N_{\text{corr}} \in [200, 400, 600]$  and  $N_{\text{up}} \in [10, 20, 30]$ , plotted against flow time  $\sqrt{8t_f}$ .
- The time taking to generate 200 configurations and flowing them  $N_{\text{flow}} = 250$  flow steps for a lattice of size  $N = 16$  and  $N_T = 32$ , with  $\beta = 6.0$  for combinations of  $N_{\text{corr}} \in [200, 400, 600]$  and  $N_{\text{up}} \in [10, 20, 30]$ .
- What we see is that increasing  $N_{\text{up}}$  is a cheaper alternative compared to using  $N_{\text{corr}}$

## Optimizing the gauge configuration generation



- We run for different values for  $N_{\text{up}}$  and  $N_{\text{corr}}$  to see what gives optimizes **computational cost** and **autocorrelation**.
- The integrated autocorrelation time for topological charge  $\langle Q \rangle$  for a lattice of size  $N = 16$  and  $N_T = 32$  with  $\beta = 6.0$  for combinations of  $N_{\text{corr}} \in [200, 400, 600]$  and  $N_{\text{up}} \in [10, 20, 30]$ , plotted against flow time  $\sqrt{8t_f}$ .
- The time taking to generate 200 configurations and flowing them  $N_{\text{flow}} = 250$  flow steps for a lattice of size  $N = 16$  and  $N_T = 32$ , with  $\beta = 6.0$  for combinations of  $N_{\text{corr}} \in [200, 400, 600]$  and  $N_{\text{up}} \in [10, 20, 30]$ .
- What we see is that increasing  $N_{\text{up}}$  is a cheaper alternative compared to using  $N_{\text{corr}}$

- Unit testing. SU(3), SU(2) multiplications.

- **Unit testing.** SU(3), SU(2) multiplications.
- **Integration testing.** Random matrix generation, lattice objects, parallelization, ect.

- **Unit testing.** SU(3), SU(2) multiplications.
- **Integration testing.** Random matrix generation, lattice objects, parallelization, ect.
- **Validation testing.** Cross checking results with a configuration from Chroma.

## Verifying the integration

- The values we will test the integrator against.

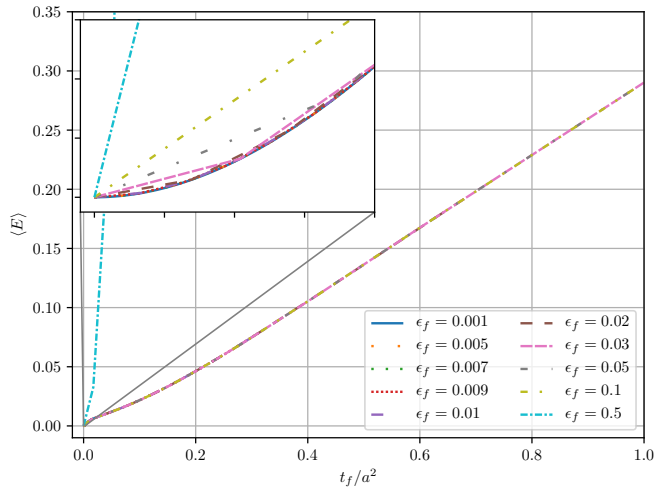
Testing the integrator for different integration steps  $\epsilon_f$ .

$\epsilon_f$	0.001	0.005	0.007	0.009	0.01	0.02	0.03	0.05	0.1	0.5
--------------	-------	-------	-------	-------	------	------	------	------	-----	-----

## Verifying the integration

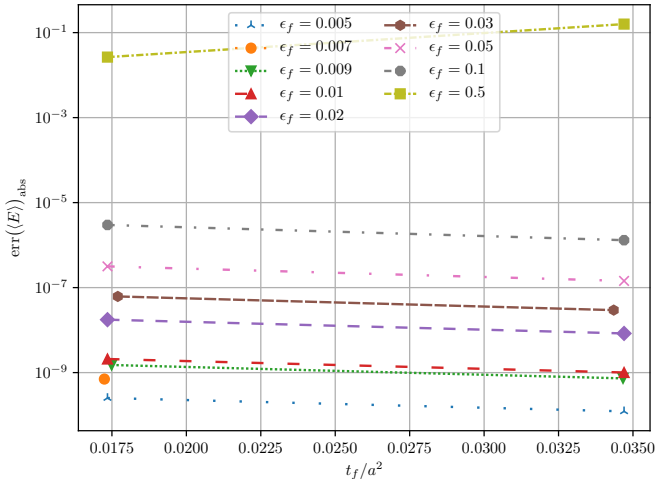
Lattice size  $N^3 \times N_T = 24^3 \times 48$  with  $\beta = 6.0$ .

- The values we will test the integrator against.
- The energy flowed for different the different  $\epsilon_f$  values.



## Verifying the integration

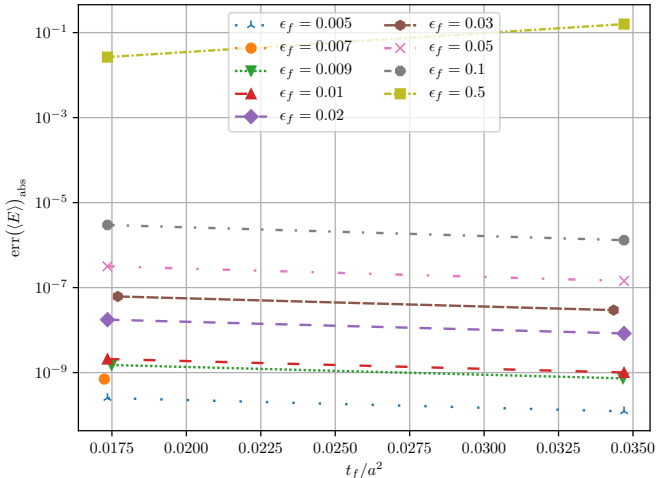
The absolute difference between the smallest flow time  $\epsilon_f = 0.001$  and those shown previously.



- The values we will test the integrator against.
- The energy flowed for different the different  $\epsilon_f$  values.
- The absolute difference between the smallest flow time  $\epsilon_f = 0.001$  and those listed in previous table.
- The reason for **only having two points** is due to the fact that we are only **comparing points that are close to each other in flow time**. If we were to have more points, we would have to double the number of flow time steps for the smallest lattices.

## Verifying the integration

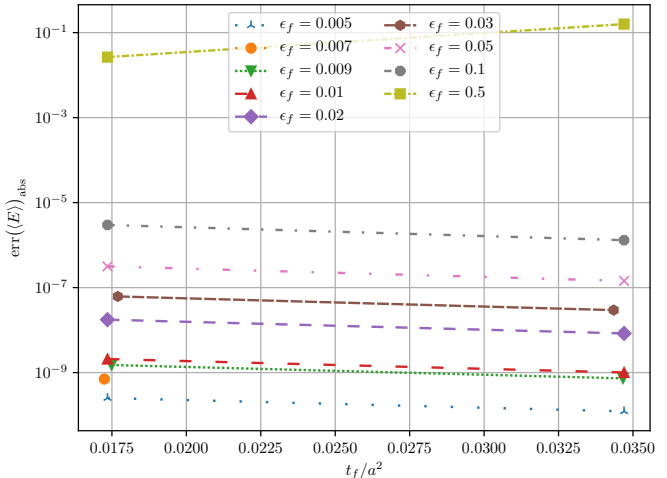
The absolute difference between the smallest flow time  $\epsilon_f = 0.001$  and those shown previously.



- The values we will test the integrator against.
- The energy flowed for different the different  $\epsilon_f$  values.
- The absolute difference between the smallest flow time  $\epsilon_f = 0.001$  and those listed in previous table.
- The reason for **only having two points** is due to the fact that we are only **comparing points that are close to each other in flow time**. If we were to have more points, we would have to double the number of flow time steps for the smallest lattices.
- An **example** of the flowing, can be seen by observing the **energy evolving over flow time**.

## Verifying the integration

The absolute difference between the smallest flow time  $\epsilon_f = 0.001$  and those shown previously.



- The values we will test the integrator against.
- The energy flowed for different the different  $\epsilon_f$  values.
- The absolute difference between the smallest flow time  $\epsilon_f = 0.001$  and those listed in previous table.
- The reason for **only having two points** is due to the fact that we are only **comparing points that are close to each other in flow time**. If we were to have more points, we would have to double the number of flow time steps for the smallest lattices.
- An **example** of the flowing, can be seen by observing the **energy evolving over flow time**.

# The non-linearity of QCD

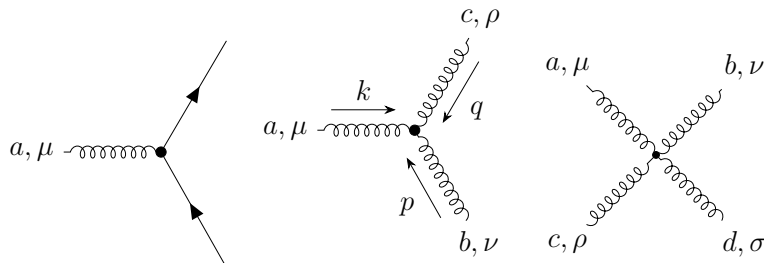
The QCD Lagrangian

$$\mathcal{L}_{\text{QCD}} = \sum_{f=1}^{N_f} \bar{\psi}^{(f)} \left( i \not{D} - m^{(f)} \right) \psi^{(f)} - \frac{1}{4} G_{\mu\nu}^a G^{a\mu\nu},$$

with action

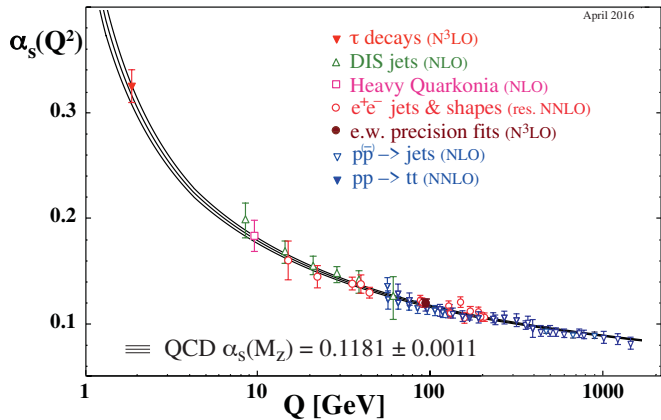
$$S = \int d^4x \mathcal{L}_{\text{QCD}}, \quad (1)$$

is invariant under a SU(3) symmetry.



- *Gluon self-interaction.*
- This central aspect is mostly covered in the pure-gauge/Yang-Mills section of the theory.
- **Two important features:** confinement and asymptotic freedom.

# Asymptotic freedom



- The coupling constant **decreases** as we **increase** the energy.
- Also serves as an *experimental proof* of QCD.
- Other lines of evidence: triple  $\gamma$  decay and muon cross section ratio  $R$ .
  - Triple  $\gamma$  decay: the number of colors is included in the cross section, which can be measured experimentally.
  - Muon cross section ratio  $R$ : the ratio is dependent on having three colors.

- We rewrite the equations slightly,

With

$$\dot{V}_{t_f} = -g_S^2 \{ \partial_{x,\mu} S_G[V_{t_f}] \} V_{t_f} = Z(V_{t_f}) V_{t_f},$$

## Solving gradient flow with Runge-Kutta 3

With

$$\dot{V}_{t_f} = -g_S^2 \{ \partial_{x,\mu} S_G[V_{t_f}] \} V_{t_f} = Z(V_{t_f}) V_{t_f},$$

and  $Z_i = \epsilon_f Z(W_i)$  we get

$$W_0 = V_{t_f},$$

$$W_1 = \exp \left[ \frac{1}{4} Z_0 \right] W_0,$$

$$W_2 = \exp \left[ \frac{8}{9} Z_1 - \frac{17}{36} Z_0 \right] W_1,$$

$$V_{t_f + \epsilon_f} = \exp \left[ \frac{3}{4} Z_2 - \frac{8}{9} Z_1 + \frac{17}{36} Z_0 \right] W_2,$$

with coefficients from Lüscher [2010].

- We rewrite the equations slightly,

- and use a structure preserving integrator with coefficients from Lüscher [2010].

## Solving gradient flow with Runge-Kutta 3

With

$$\dot{V}_{t_f} = -g_S^2 \{ \partial_{x,\mu} S_G[V_{t_f}] \} V_{t_f} = Z(V_{t_f}) V_{t_f},$$

and  $Z_i = \epsilon_f Z(W_i)$  we get

$$W_0 = V_{t_f},$$

$$W_1 = \exp \left[ \frac{1}{4} Z_0 \right] W_0,$$

$$W_2 = \exp \left[ \frac{8}{9} Z_1 - \frac{17}{36} Z_0 \right] W_1,$$

$$V_{t_f + \epsilon_f} = \exp \left[ \frac{3}{4} Z_2 - \frac{8}{9} Z_1 + \frac{17}{36} Z_0 \right] W_2,$$

with coefficients from Lüscher [2010].

- We rewrite the equations slightly,
- and use a structure preserving integrator with coefficients from Lüscher [2010].
- We control the accuracy of this integrator by  $\epsilon_f$ .

## Solving gradient flow with Runge-Kutta 3

With

$$\dot{V}_{t_f} = -g_S^2 \{ \partial_{x,\mu} S_G[V_{t_f}] \} V_{t_f} = Z(V_{t_f}) V_{t_f},$$

and  $Z_i = \epsilon_f Z(W_i)$  we get

$$W_0 = V_{t_f},$$

$$W_1 = \exp \left[ \frac{1}{4} Z_0 \right] W_0,$$

$$W_2 = \exp \left[ \frac{8}{9} Z_1 - \frac{17}{36} Z_0 \right] W_1,$$

$$V_{t_f + \epsilon_f} = \exp \left[ \frac{3}{4} Z_2 - \frac{8}{9} Z_1 + \frac{17}{36} Z_0 \right] W_2,$$

with coefficients from Lüscher [2010].

- We rewrite the equations slightly,
- and use a structure preserving integrator with coefficients from Lüscher [2010].
- We control the accuracy of this integrator by  $\epsilon_f$ .

## Additional ensembles

- Additional ensembles made in order to illuminate additional aspects of the topological charge.
- Supporting ensembles made on Smaug. All ensembles were flown  $N_{\text{flow}} = 1000$  steps with  $\epsilon_{\text{flow}} = 0.01$ .

Ensemble	$N$	$N_T$	$N_{\text{cfg}}$	$N_{\text{corr}}$	$N_{\text{up}}$	$a$ [fm]	$L$ [fm]
$E$	8	16	8135	600	30	0.0931(4)	0.745(3)
$F$	12	24	1341	200	20	0.0931(4)	1.118(5)
$G$	16	32	2000	400	20	0.0790(3)	1.265(6)

## Energy definition

We use  $t_0$

$$E = \frac{a^4}{2|\Lambda|} \sum_{n \in \Lambda} \sum_{\mu, \nu} (F_{\mu\nu}^{\text{clov}}(n))^2$$

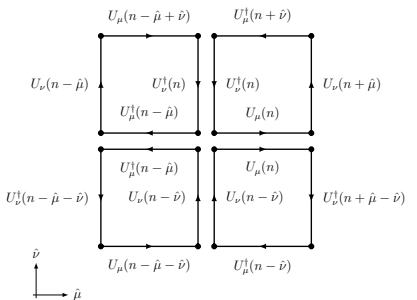
- Defined as the field strength tensor squared averaged over all lattice points and directions.

## Energy definition

We use  $t_0$

$$E = \frac{a^4}{2|\Lambda|} \sum_{n \in \Lambda} \sum_{\mu, \nu} (F_{\mu\nu}^{\text{clov}}(n))^2$$

$F_{\mu\nu}^{\text{clov}}(n)$  is given by



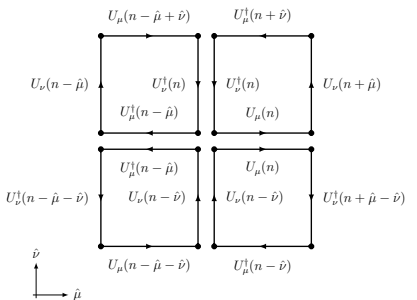
- Defined as the field strength tensor squared averaged over all lattice points and directions.
- We will use the clover field strength definition in gauge observables.
- Symmetries** will allow us to **reduce** the effective **number of clovers** need to **calculate from 24 to 6**.

## Energy definition

We use  $t_0$

$$E = \frac{a^4}{2|\Lambda|} \sum_{n \in \Lambda} \sum_{\mu, \nu} (F_{\mu\nu}^{\text{clov}}(n))^2$$

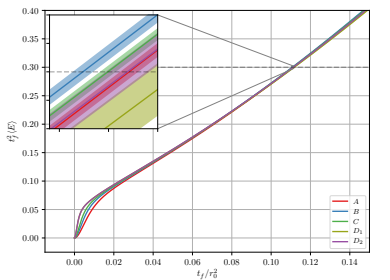
$F_{\mu\nu}^{\text{clov}}(n)$  is given by



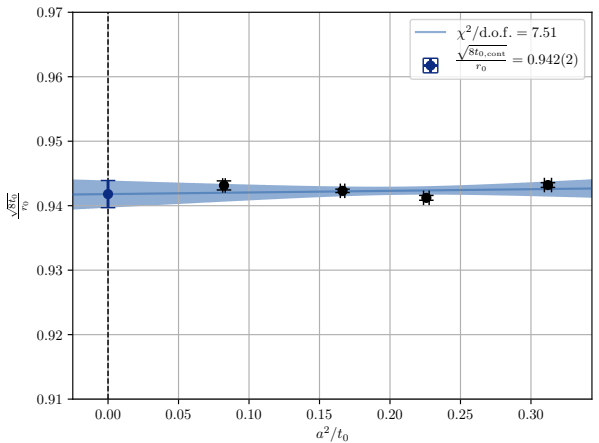
- Defined as the field strength tensor squared averaged over all lattice points and directions.
- We will use the clover field strength definition in gauge observables.
- Symmetries** will allow us to **reduce** the effective **number of clovers** need to **calculate from 24 to 6**.

Using scale definition  $t_0$  from Lüscher [2010],

$$\{t_f^2 \langle E(t) \rangle\}_{t_f=t_0} = 0.3.$$



## Scale setting $t_0$



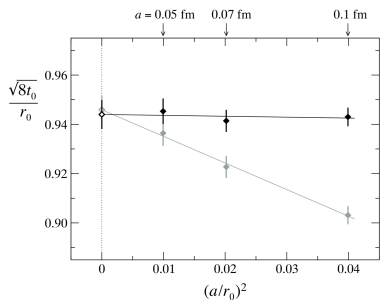
Continuum extrapolation using ensembles  $A$ ,  $B$ ,  $C$ , and  $D_2$  gives  
 $t_0,\text{cont}/r_0^2 = 0.11087(50)$ .

- The continuum extrapolation  $a \rightarrow 0$  for  $t_0$  of the four ensembles  $A$ ,  $B$ ,  $C$ , and  $D_2$ .
-

## Scale setting $t_0$

- The continuum extrapolation  $a \rightarrow 0$  for  $t_0$  of the four ensembles  $A$ ,  $B$ ,  $C$ , and  $D_2$ .
- $r_0 = 0.5$  fm.

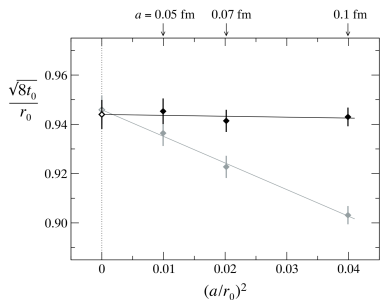
This matches the values retrieved by Lüscher [2010],



## Scale setting $t_0$

- The continuum extrapolation  $a \rightarrow 0$  for  $t_0$  of the four ensembles  $A$ ,  $B$ ,  $C$ , and  $D_2$ .
- $r_0 = 0.5$  fm.

This matches the values retrieved by Lüscher [2010],



## Scale setting $t_0$

Ensemble	$L/a$	$L$ [fm]	$a$ [fm]
$A$	24	2.235(9)	0.0931(4)
$B$	28	2.214(10)	0.0791(3)
$C$	32	2.17(1)	0.0679(3)
$D_1$	32	1.530(9)	0.0478(3)
$D_2$	48	2.29(1)	0.0478(3)

## Scale setting $t_0$

- Extrapolation results for  $t_0$ , where we retrieved the exact point of intersection between  $t_f^2 \langle E \rangle$  and 0.3 using  $N_{\text{bs}} = 500$  bootstrap fits. Extrapolating to the continuum gives us  $t_{0,\text{cont}}/r_0^2 = 0.11087(50)$ .

Ensemble	$t_0[\text{fm}^2]$	$t_0/a^2$	$t_0/r_0^2$
$A$	0.02780(2)	3.20(3)	0.11121(9)
$B$	0.02769(2)	4.43(4)	0.11075(10)
$C$	0.02775(2)	6.01(6)	0.11099(8)
$D_1$	0.02779(5)	12.2(1)	0.1112(2)
$D_2$	0.02794(9)	12.2(1)	0.1117(3)

## Scale setting $t_0$

- Extrapolation results for  $t_0$ , where we retrieved the exact point of intersection between  $t_f^2 \langle E \rangle$  and 0.3 using  $N_{\text{bs}} = 500$  bootstrap fits. Extrapolating to the continuum gives us  $t_{0,\text{cont}}/r_0^2 = 0.11087(50)$ .

Ensemble	$t_0[\text{fm}^2]$	$t_0/a^2$	$t_0/r_0^2$
$A$	0.02780(2)	3.20(3)	0.11121(9)
$B$	0.02769(2)	4.43(4)	0.11075(10)
$C$	0.02775(2)	6.01(6)	0.11099(8)
$D_1$	0.02779(5)	12.2(1)	0.1112(2)
$D_2$	0.02794(9)	12.2(1)	0.1117(3)

## Scale setting $t_0$

- Notice the  $\chi^2/\text{d.o.f.}$  of the extrapolation versus the two other extrapolations.

Extrapolations for different ensemble-combinations

Ensembles	$t_{0,\text{cont}}/r_0^2$	$\chi^2/\text{d.o.f.}$
$A, B, C, D_2$	0.11087(50)	7.51
$B, C, D_2$	0.1115(3)	0.41
$A, B, C, D_1$	0.1119(6)	0.88

## Scale setting $w_0$

Can also set a scale using the derivative which offers more granularity for small flow times,

$$W(t)|_{t=w_0^2} = 0.3,$$

$$W(t) \equiv t_f \frac{d}{dt_f} \{ t_f^2 \langle E \rangle \}.$$

First presented by Borsanyi et al. [2012].

## Scale setting $w_0$

Ensembles	$w_{0,\text{cont}}[\text{fm}]$	$\chi^2/\text{d.o.f}$
$A, B, C, D_2$	0.1695(5)	7.12
$B, C, D_2$	0.1702(3)	0.53
$A, B, C, D_1$	0.1706(6)	0.86

Ensembles	$w_{0,\text{cont}}[\text{fm}]$	$\chi^2/\text{d.o.f}$
$A, B, C, D_2$	0.1695(5)	7.12
$B, C, D_2$	0.1702(3)	0.53
$A, B, C, D_1$	0.1706(6)	0.86

Comparable to Borsanyi et al. [2012] which included dynamical fermions, with  $w_{0,\text{cont}} = 0.1755(18)(04)$  fm.

## Autocorrelation in the energy

The autocorrelation of the energy. A value of  $\tau_{\text{int}} = 0.5$  indicates that we have zero autocorrelation.

